The role of talus size distribution & the frequency of transport in wide and narrow valleys on bedrock valley widening: Buffalo National River, Arkansas

by

Olivia Hermine Groeber

B.S., University of Arkansas, 2020

A THESIS

submitted in partial fulfillment of the requirements for the degree

MASTER OF SCIENCE

Department of Geography and Geospatial Sciences
College of Arts and Sciences

KANSAS STATE UNIVERSITY
Manhattan, Kansas

2022

Approved by:

Major Professor
Dr. Abigail L. Langston

Copyright

Abstract

Bedrock river valleys are a valuable resource from which we learn about historic climactic changes, shifts in discharge and sediment inputs, movement of the river channel, and bedrock valley widening processes. Bedrock river valleys are often found in two end-member states: narrow, canyon-like bedrock valleys, and wide, bedrock valleys many times wider than the river channel. So far, little research has been done to determine the controls on bedrock river widening. Previous work has pointed to lithology and upstream drainage area as the main controls on bedrock valley width, but these do not take into account specific valley widening processes. I tested a conceptual model describing two end-member processes to create bedrock river valleys. First, the river laterally erodes and undercuts the bedrock valley wall, eventually leading to collapse. Second, the river transports the collapsed talus blocks and moves them from the wall, allowing the river access to the wall again for continued undercutting. If a river at different flow regimes cannot move a talus block, the valley wall is shielded from lateral erosion until the grain size is small enough to be moved, thus preventing bedrock valley widening. The Buffalo River is an ideal bedrock river to address this question as it has both wide and narrow bedrock valleys in similar lithologies. I measured the grain sizes of talus blocks at the base of bedrock valley walls, grain sizes of bedload, and bankfull width at 40 sites in wide and narrow valleys. If talus block size contributes to the development of wide bedrock valleys, I would expect that I would find large talus in the narrow valley and smaller talus grains in the wide valley. Locations in the narrow valleys have larger talus grain sizes than locations in the wide bedrock valleys for our field site in Buffalo National River. The wide valleys had a greater ability to move talus blocks in the 100 and 1,000-year floods, but I found that the narrow valleys

could hardly move talus grains even in the 1,000-year floods. These results support the conceptual model that talus block size, in conjunction with many other factors, is a control on bedrock valley width.

Table of Contents

List of Figures

List of Tables

Acknowledgements

I am extremely grateful to Abigail L. Langston, my advisor, for her patient guidance during the countless hours of research design and execution, trouble shooting, and writing revisions. I could not have asked for a better mentor; Dr. Langston was always available to provide professional and personal guidance. I would also like to thank my committee members, Dr. Arnaud Temme, Dr. Jill Marshall, and Dr. Chuck Martin, for their insight and counsel during my masters' thesis. My work in the Buffalo National River was made possible through funds provided by the Steve Kale Fellowship and Kansas State University Department of Geography and Geospatial Sciences.

I am also very grateful to Clay Robertson, a co-researcher, PhD candidate, and friend. We took many trips to Buffalo National River gathering data and braving less than ideal conditions. His encouragement in stories and conversation have meant a lot to me, and I wish him the best in his continued research.

Finally, I want to thank the people who support me in my day to day life. I forget the need I have for community around me, and am thankful to my small community who have accepted me as I am. To Landry, my parents, and siblings, thank you for your love and support from day one. I cannot write adequate words to let each of you know the life your words and actions bring to my daily life. From my heart to yours thank you.

Chapter 1 - **Introduction**

Bedrock river valleys can exist in a variety of states ranging from wide to narrow. For our purposes we consider a wide valley to be many times (10x's) larger than the river channel is wide. For a narrow bedrock river valley we determined that the valley is no more than a few times wider than the channel width (Langston & Tucker, 2018). We want to better understand the controls on bedrock valleys widening, specifically what keeps some valleys narrow and what allows some valleys to widen. This is important for many reasons, including but not limited to the health of river valley ecosystems and habitats (Beeson et al., 2018; May et al., 2013; Sweeney et al., 2004), flood hazards (Sampson et al., 2015), and river incision into mountain ranges (Yanites, 2018; Yanites et al., 2010).

A new conceptual model, proposed by Langston and Tucker (2018) and Langston and Temme (2019), describes a two-step process for bedrock river valley widening. First, a bedrock river undercuts the adjacent valley wall, via lateral erosion, and the wall collapses under its own weight. The collapsed pile of talus blocks can be small or large in size, depending on lithological characteristics of the collapsed material. Next, the river must transport the collapsed material. If the river can transport collapsed material away from the valley wall rapidly, the river can access the wall more frequently, widening the valley. If the collapsed material is too large or too voluminous for the river to transport rapidly, blocks sit at the base of the wall, protecting it from undercutting. Before large blocks can be transported, weathering processes need to take place, making the collapsed material smaller. In this study, we explore whether this protection of the valley wall by collapsed material plays a role in keeping the bedrock valley narrow.

While many studies have focused on vertical incision (e.g., Beer & Turowski, 2015; Brocard & Van Der Beek, 2006; Bufe et al., 2017; Sklar & Dietrich, 2004; Whippleet al., 2000), lateral bedrock erosion has been largely understudied until recently (Fuller et al., 2016; Hancock & Anderson, 2002; Li et al., 2020). Rivers can vertically incise and laterally erode simultaneously or individually. What makes a river shift from one to the other is not fully understood; we know that the balance between water flux and sediment flux can determine how a river shifts between lateral and vertical erosion. Changes between water and sediment flux occur during changes in climate and tectonics. If climate and/ or tectonics control when river incision or lateral widening occurs, then bedrock valleys and strath terraces can tell us about river conditions at different times in the past. The current understanding of lateral bedrock erosion is based on numerical modeling and flume experiments, leaving many more opportunities for research (Beer et al., 2017; Bufe et al., 2017; Fuller et al., 2016; Hancock & Anderson, 2002; Li et al., 2020; Tomkin et al., 2003).

We also know that valley width should scale with drainage area (Brocard & Van Der Beek, 2006; Langston & Temme, 2019; Thaler & Covington, 2016), and that in many scenarios valley width depends on lithology (Johnson & Finnegan, 2015; Schanz et al., 2018). Drainage area and lithology each are important to bedrock river valley width, but they do not explain how the valley develops. We want to understand how different types of valleys develop through time in different lithologies as a more complete way to test the proposed conceptual model of valley widening (Langston & Temme, 2019; Langston & Tucker, 2018). In light of the lack of research on bedrock river valley widening, we went out to Buffalo National River to collect field data to answer a few fundamental questions.

In the Buffalo River we were interested in the frequency of potential talus block transport from the base of bedrock valley walls in wide and narrow valleys. I gathered field measurements of talus grain sizes, bedload grain sizes, and channel widths at 40 site locations, 26 in the Main Stem Buffalo River and 14 in the Little Buffalo River, a tributary. I found that there was a significant difference in grain size between the wide and narrow valleys. The talus grain size measurements in conjunction with historic discharge data provided by U.S. Geological Survey (USGS) allowed me to calculate the potential for movement of specific grain sizes per site location for the 2-year, 100-year, and 1,000-year flood events (Moore, 2014; U. S. Geological Survey, 2020). I found that these calculations provided an insight into whether grains were potentially shielding the valley wall from widening.

1.1 Overarching Goal

The broad goal of this research is to *quantify grain sizes* of talus blocks and bedload *in wide and narrow valleys* to determine *how frequently* the river has the *potential to move them*.

1.2 Research Questions

1. What is the grain size distribution of talus piles in wide valleys versus narrow valleys in the Buffalo National River?

I am interested in grain size distributions in talus piles in both the wide and narrow bedrock valleys. I expect the narrow bedrock valleys to will have large talus blocks that protect the walls, while the wide bedrock valleys will have smaller talus blocks that can be more easily transported.

2. How does bankfull and peak basal shear stress change going downstream?

Moving downstream, we would expect that the river channel widens while the slope decreases. With wider channels and lower slopes the basal shear stress also decreases, but this is in conjunction with increased discharge downstream.

3. What size flood can potentially transport D50 and D84 talus grain sizes?

I calculated critical shear stress for D50 and D84 talus grain sizes at each sample location. I then compared these critical shear stresses with calculated basal shear stresses in order to determine the likelihood of talus transport during the 2-year, 100-year, and 1,000-year floods.

Chapter 2 - **Background**

2.1 Vertical Incision

Vertical incision in bedrock rivers has been extensively studied quantitatively for about 30 years (Beer & Turowski, 2015; Brocard & Van Der Beek, 2006; Bufe et al., 2017; Howard, 1994; Sklar & Dietrich, 2004; Whipple et al., 2000). Vertical bedrock incision has been modeled using the stream power equation.

$$\frac{dz}{dt} = KA^m S^n \qquad \text{Equation 1}$$

This equation describes the erosive power of a bedrock river (Whipple et al., 2000; Whipple & Tucker, 1999). Here bedrock erosion rate is a function of drainage area (*A*), slope (*S*), and an erodibility coefficient, *K*, that accounts for effects of both lithology and climate. *m* and *n* are exponents.

Thresholds of shear stress are used to model whether a river is flowing strong enough to pluck blocks in a bedrock river (Whipple et al., 2013). Shear stress is the erosive power of the river exerted on the bed that must exceed a threshold for bedload material to move. The bedrock erosion equation with a threshold shear stress term is as follows (Equation 2). It describes the requirement that basal shear stress must be greater than the critical shear stress to pluck blocks from the bed or transport sediment covering the bed.

$$\boldsymbol{\frac{dz}{dt} = K(\tau - \tau_{crit})^a} \qquad \text{Equation 2}$$

In this equation *K* is bedrock erodibility, τ is basal shear stress, τ_{crit} is the critical shear stress necessary to pluck bedrock or transport sediment, and *a* is an exponent that is equal to 3/2 or 1 depending on whether you are using shear stress, 3/2, or unit stream power, 1.

Rivers cannot incise bedrock riverbeds if the flow is not strong enough to pluck/ move blocks. If there is excess shear stress, a critical threshold will be surpassed, and plucking can occur (Turowski et al., 2008). Whipple et. al (2000) describes plucking, fluting/ potholing as the most efficient form of bedrock erosion in the fluvial system at both local and reach scale, but it occurs much less frequently than other forms of bedrock erosion (Whipple et al., 2013). Abrasion is the process of saltating bedload impacting bedrock, slowly wearing away at the rock; one could think of sandblasting to better understand what abrasion is and does. Sklar and Dietrich (2004), proposed a "tools and cover" model to describe the erosional efficiency of a river in response to the amount of sediment that a river can carry. Sediment, is the "tool" responsible for bedrock erosion through abrasion. Although, if sediment exceeds the capacity the river can carry, "cover" occurs as sediment is deposited on the bed. If the bed is covered, the river is unable to vertically incise. Without access to the riverbed there is no potential for lateral bedrock erosion to occur.

2.2 Lateral Erosion

Lateral erosion is less studied than vertical incision. Lateral erosion is important for understanding the mechanisms to explain the past formation of strath terraces, to predict future widening processes, and understand the connections between hillslope and lateral erosion processes (Foster et al., 2017; Hancock & Anderson, 2002; Langston & Tucker, 2018; Sklar et al., 2017). Strath terraces are flat bedrock surfaces that have been laterally eroded by rivers and then incised, leaving the flat river-carved area that are capped with fluvial sediments. Strath terraces represent river elevations of the past, allowing us to see signatures of different events and processes occurring to create strath terraces, events including but not limited to shifts in climate, tectonic activity, and anthropogenic controls like damming. This is valuable because the history of strath terraces can suggest the factors at play creating wide bedrock valleys for the duration of bedrock valley formation.

Lateral erosion, therefore, can give understanding and context to the timespan on how rivers shape valleys, allowing us to model how bedrock river valleys widen on a larger scale, and allow for better understand of aquatic ecosystem stability and function (Beeson et al., 2018; May et al., 2013).

In order for bedrock valley widening to occur, periods of lateral erosion must be greater than the periods of vertical incision (Hancock & Anderson, 2002). River channels laterally erode, ultimately widening the bedrock river valleys. There must be a distinction made between lateral bedrock erosion and bedrock valley widening. Lateral bedrock erosion is the small-scale process that occurs on rock surfaces of the river channel banks due to abrasion or plucking. Lateral bedrock erosion of channel walls often occurs at rates of millimeters per year (Beer et al., 2017; Bufe et al., 2017; Fuller et al., 2016; Marcotte et al., 2021). Lateral erosion on the bank continues until the river undercuts the bank and it collapses under its own weight. After the valley wall collapses and the collapsed pile of overlying wall material is fully transported away, the bedrock wall is then again exposed to the river for the small-scale lateral erosion to laterally cut or erode the bedrock valley wall again.

Bedrock lateral erosion has been studied using numerical and experimental models, since the timescale for lateral erosion is generally too long to observe in field, dependent upon the hardness of the bedrock wall studied. In an experimental flume study, Fuller et al. (2016) found that increased bed roughness increased the rate of lateral erosion. The reason they found that increased bed roughness increased the rate of erosion was because the bed roughness caused more particles to deflect toward the walls, eroding the walls via abrasion. Li et al. (2020) found that vertical incision occurs in a bedrock river the majority of time, but when the bed is almost fully covered, lateral erosion is the more prevalent process. Marcotte et al. (2021) measured lateral bedrock erosion rates that were tens of millimeters per year in both shale and limestone bedrock. Lateral bedrock erosion occurring in a river is a necessary component for a river valley to widen.

2.3 Controls on Vertical Incision vs. Lateral Widening

Climate is a driving factor for shifts in river discharge and/ or sediment flux (Hancock & Anderson, 2002; Schanz et al., 2018; Tucker & Bras, 2000). Climate has shifted and changed for thousands of years; those shifts have been largely responsible for changes in discharge and sediment flux. Rivers are constantly adjusting to imposed sediment and discharge to come back to an equilibrium channel (Hancock & Anderson, 2002). One example being, higher volumes of sediment in a river can cause the river to aggrade and shift the river from vertically incising to laterally eroding. Just because a river is aggrading does not mean there is always lateral erosion, the river could simply become shallower and/ or narrower with the deposition. If there is increased uplift the river has steeper slopes, this will transport more bedload meaning less sediment on the bed and increased vertical incision. In addition, if there were increases in discharge, the river would have greater ability to move more material causing greater amounts of incision (Whipple & Tucker, 1999).

Where changes in tectonics is not a factor, strath terraces show evidence of past shifts in climate caused by changes in river discharge and sediment flux (Bull, 1991; Hancock & Anderson, 2002; Schanz et al., 2018). Strath terraces are places we can see where a bedrock river has shifted from incision to lateral widening or vice versa. These strath terraces are the remnants of floodplains the river carved during one period of time and then abandoned to a lower elevation based on changes in climate, tectonic activity, volcanic activity, or human activity (Schanz et al., 2018).

Climate includes precipitation and temperature, shifts in the climactic regime of an area could greatly alter the way a river responds. Rivers use sediment to erode both vertically and/or laterally, depending on the circumstance. One climactic event that can affect whether the river is vertically or laterally eroding, is the freeze thaw cycle which can increase the sediment flux from hillslopes into a river channel, potentially changing the input of sediment into the river. Changes in fracture spacing could also occur due to freeze thaw cycles which would increase sediment flux, even many years after the initial occurrence (Marshall et al., 2015). Increases in sediment release and transport from hillslopes are directly related to temperature regime (Marshall et al., 2015). These increases in sediment flux can increase the tool contents of the river or the cover depending upon where the sediment is deposited (Sklar & Dietrich, 2004). Discharge also plays a role in how the sediment affects incision within a river. Discharge can change from a steady flood regime to a flashier flood regime based on climactic change (Tucker & Bras, 2000). This would potentially allow larger sediment blocks to be transported by the river. In terms of sediment transport, the variation in precipitation is potentially more significant than total precipitation values for a location (Tucker & Bras, 2000). Rainfall intensity, specifically, has been used for many models to describe the driving factor of increased discharge (Marshall et al., 2015). In this way, rivers are heavily influenced by climate through changes in sediment flux, and river discharge as seen historically evidenced in river strath terraces (Schanz et al., 2018).

2.4 Valley Width and Valley Widening

Previous studies have shown that there are two important factors that control valley width: discharge and lithology. Discharge is a function of the basin area that is accumulated to a certain point. Often, drainage area is used as a proxy for discharge. With larger discharges or drainage areas we usually find wider valleys (Brocard & Van Der Beek, 2006; Langston & Temme, 2019; Tomkin et al., 2003). Lithology is often cited as a main control on bedrock river valley width. Wide bedrock valleys occur more in soft lithologies than in harder lithologies (Johnson & Finnegan, 2015; Schanz & Montgomery, 2016). Wide valleys most often occur in easily erodible bedrock like weakly cemented sandstones, shales, or mudstones where slaking of bedrock material allows for rapid lateral erosion (Johnson & Finnegan, 2015; Marcotte et al., 2021; Schanz & Montgomery, 2016). Wide valleys are also commonly found in dolomite, limestone, and sandstone lithologies (Keen-Zebert et al., 2017; Langston & Temme, 2019). Lithology can be a large factor in how rocks not only physically or chemically weather but also how they break away from the massive walls to form individual blocks.

A novel conceptual model describing end members of bedrock valley widening explains variation in valley widths not accounted for by drainage area or lithology (Langston & Temme, 2019). Bedrock valley widening begins with lateral bedrock erosion on steep valley walls that are immediately adjacent to the river channel. First, the river undercuts the wall; once the overlaying material becomes too heavy, the wall collapses and forms a talus pile at the base of the valley wall (Figure 1). Next, the river must transport the collapsed material away from the valley wall for widening to continue. Collapsed material can only be transported by the river if the collapsed blocks are small enough. If blocks can be transported by river flows, the bedrock wall is exposed again to lateral erosion. If the collapsed material is too large to be transported by the river, weathering processes need to make the talus blocks smaller until they can be transported away from the valley wall by the river (Figure 1) (Langston & Temme, 2019; Langston & Tucker, 2018).

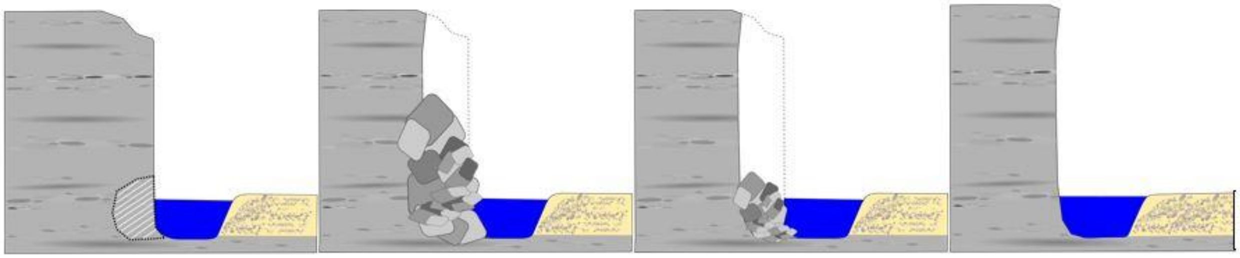

Figure 1: This shows the two-step conceptual model of collapse and transport of collapsed material to create wider bedrock river valleys. There is undercut followed by collapse. Transport then happens, but if a block is too large they must be weathered to a smaller, more transportable size. After all blocks are gone the river gains access to the valley wall for continued lateral erosion and undercutting (Langston & Temme, 2019).

2.4.1 Shear Stress

Collapsed talus blocks are transported away from valley walls by shear stress exerted on the rocks by the river. Basal shear stress is a force over an area that erodes bedrock and transports the river materials. Basal shear stress is provided by:

$$\tau_0 = \rho g H S \qquad \text{Equation 3}$$

Here τ_0 is the basal shear stress or the shear stress exerted by the river on the riverbed. Shear stress is a function of the density of water, ρ, the gravitational force, g, the height of the water profile, *H*, and the slope of the riverbed, *S*.

The lowest shear stress needed to potentially move a certain grain size is determined by the critical shear stress. The critical shear stress of a certain grain size can be calculated using this equation:

$$\tau_c = \theta(\rho_s - \rho_f) g D \qquad \text{Equation 4}$$

Critical shear stress, τ_c, non-dimensional Shields parameter, θ, density of rock minus the density of water, $(\rho_s - \rho_f)$, gravitational force, g, and the diameter of grain size of the material being moved, *D*. Movement of a grain can occur when the critical shear stress is met or exceeded. If talus blocks falling in the river are relatively small, they are more easily or more frequently transported by the river compared to larger blocks in the same river at the same location. Theoretically, the valley widens faster when collapsed material is completely moved from the wall, and the river has access to the bedrock wall allowing for more frequent exposure to erosion (Langston & Temme, 2019; Langston & Tucker, 2018). If talus material is larger and the shear stress is not large enough to move those blocks, the talus stays in place longer, preventing the valley from widening until transport away from the bottom of the bluff wall occurs.

2.5 Grain Sizes in the Channel

The grain sizes in and near river channels tell the story of flow conditions occurring in that location. The river is constantly re-arranging the bedload material and changing the channel morphology (Eaton et al., 2020; MacKenzie et al. , 2018). Areas of low velocity have areas of deposition; at these locations we find gravel bars. These are areas where large floods have left blocks that were moved during high flow events. Areas with little to no bedload (areas with exposed bedrock) are areas the river has been able to move the material that was on the surface. This means that there may be vertical erosion or incision of the riverbed. We look at bedload grain size distributions to determine what grain sizes a river can transport under specific flow conditions.

Grain sizes in a river change depending upon scale being discussed and quite often so does the lithology of the river system. Fining occurs in the downstream direction, due to selective sorting and downstream abrasion (Attal et al., 2015; Knighton, 1998). Over kilometers we see that a river's grain distributions will change from generally larger grains to smaller grains; we generally would observe larger grains in the steeper upstream sections and in the wider flatter downstream sections of the river we generally have smaller grains (Sklar et al., 2017). Within a shorter distance, hundreds of meters, we may not expect much change in grain size distribution. There may be areas where the downstream fining trend is disrupted, areas where there are sediment inputs from tributaries or hillslopes (Bull, 1991; Knighton, 1998; Sklar et al., 2017). The lithology going downstream can change, creating lithologic knickpoint locations that can either increase or decrease the grain size of rocks entering the river (Johnson & Finnegan, 2015; Menting et al., 2015).

The bedload grain size that determines the stability or instability of a channel in a river system is the D50 (Attal & Lavé, 2006; Eaton et al., 2020). However the transport threshold of the D95 grain size is better able to change channel stability, suggesting river channel shape change and perhaps increased mobilization for widening with grains of that size or smaller (Eaton et al., 2020). The D84 is the grain size where 84 percent of the other grains are smaller; it is often used as the largest grain size that can be moved in larger flood events (Knighton, 1998).

Chapter 3 - **Field Site**

3.1 Field Site Description

My research site is located in the western portion of Buffalo National River (Figure 2) in north central Arkansas. The drainage area for the Buffalo River watershed is ~3,468 km^2, and the main stem of the channel runs ~238 km long, from the headwaters to the confluence with the White River. The climate is humid with an average annual precipitation of ~120 cm/ yr, with most precipitation occurring during the mid-spring to early summer months. The river discharge is strongly characteristic of the rain events that occur in the area, with sporadic rain events that give the river a very flashy discharge regime. In Figure 3, I show two years of data to illustrate the typical seasonal changes in discharge even though the historical gauges have much larger data sets. The peaks of the hydrograph display the rise with an intense sharpness which quickly dissipates in an almost equally steep slope (Figure 3). Those peaks correspond to precipitation events in the Buffalo River area. Since the discharge is closely tied to precipitation, we see that there is high discharge in the spring and summer months with low discharge in the late summer into the fall/ winter months (Figure 3). In Table 1, maximum discharges that have been recorded at four USGS river gauges and the discharges for a 2-year flood event. A 2-year flood has a 50 percent chance of happening in a particular year. The maximum discharges are during much larger events, giving context to what has historically happened on the river at these locations.

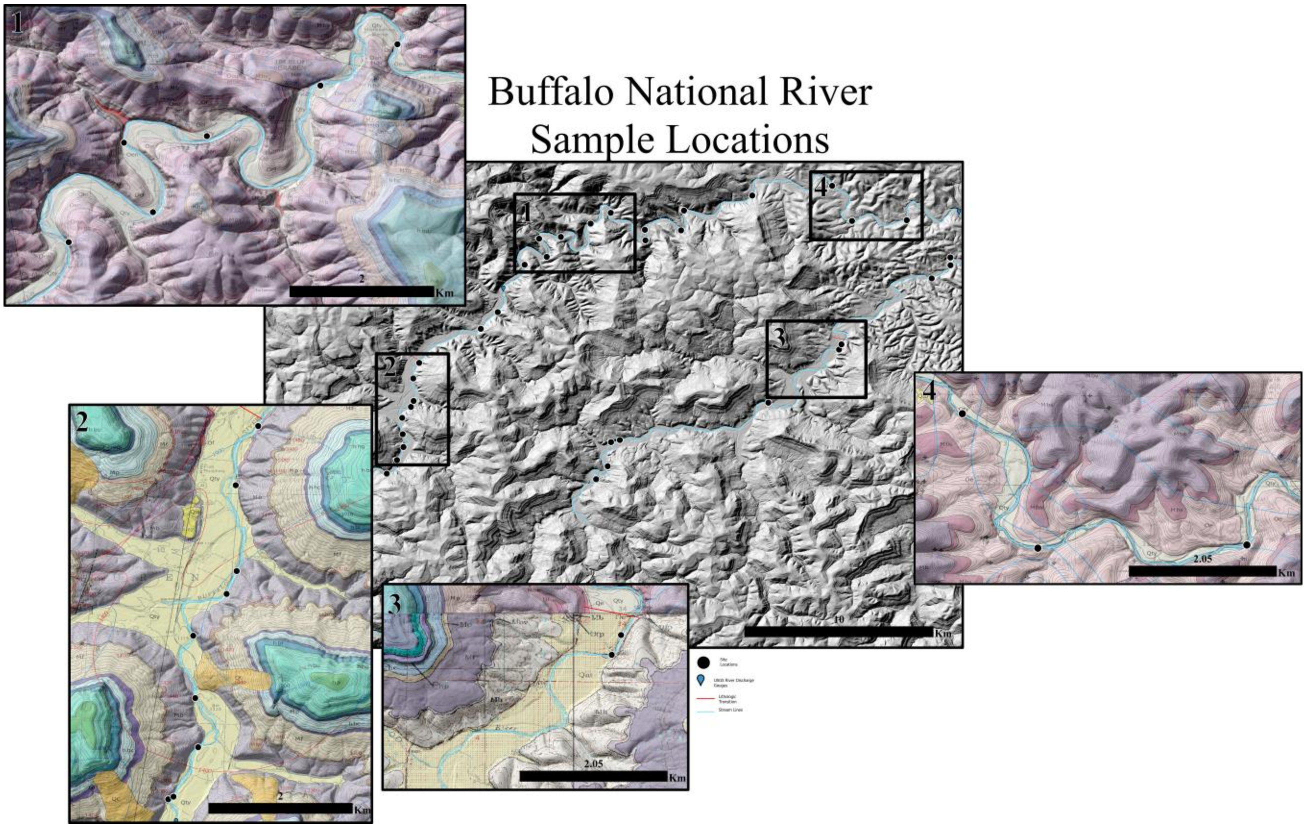

Figure 2: Most site locations (black dots) in Buffalo National River along with USGS river discharge gauges (light blue pins) on lithologic maps. The Boone and Everton Formations have red transition lines differentiating where the shift in lithology occurs.

1: This is the Ponca area where we find many of our narrow valleys, Everton Formation.

2: This is Boxley Valley containing some of my most upstream site locations in the wide river valley, Boone Formation.

3: This is part of the Little Buffalo River a southern tributary of the Buffalo River. This section of the river are wide valleys in the Boone Formation.

4: These sites are closest to the Pruitt USGS river gauge in the narrow valleys, Everton Formation.

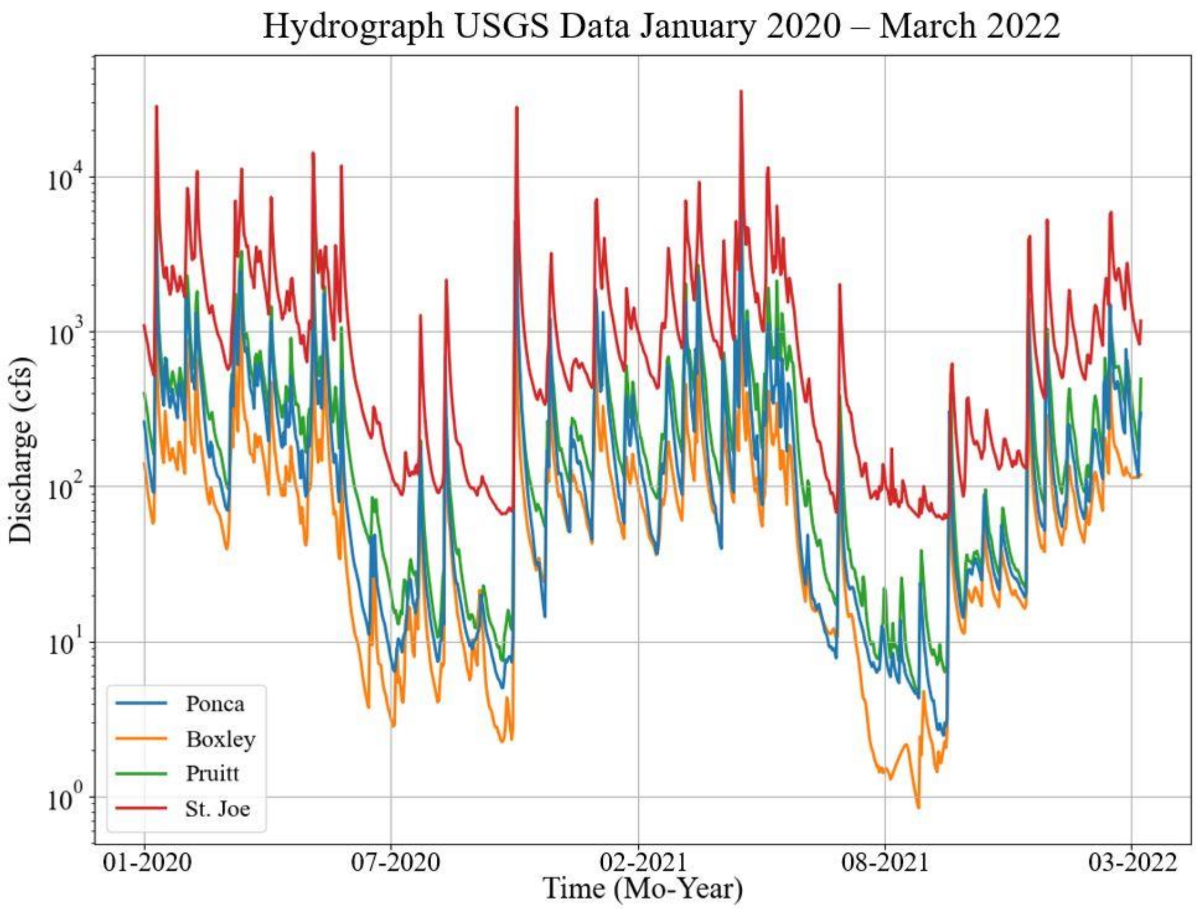

Figure 3: Hydrograph of the Boxley, Ponca, Pruitt, and St. Joe gauging stations over a two year three month period (USGS, 2022). Discharge, y-axis, is in m^3/s in log scale, and time is on the x-axis in mo-year intervals (2020-2022). This shows discharge for the two years I was collecting data from Buffalo River; the gauging stations have much more historical discharge data than is represented here. This hydrograph displays that the yearly cycle of flashy discharge in the Buffalo River is due to precipitation events occurring in the area.

Gauge	Maximum Discharge (m^3/s)	2-Year Flood Discharge (m^3/s)
Boxley	821	280
Ponca	1104	396
Pruitt	762	402
St. Joe	4474	1093

Table 1: Four USGS river gauges within the Buffalo River study area. The maximum historically recorded discharge is provided in m^3/s along with the 2-year flood discharge in m^3/s (USGS, 2022).

In the Buffalo River both wide and narrow bedrock valleys exist (Figure 4). The wide river valleys range from 500 m to over 1,500 m at some of the widest sections (Figure 4). A narrow valley is only a fraction of the size of a wide valley, and ranges from 100 m to 250 m wide (Figure 4). The wide valleys are often present in the Boone Formation in the headwaters of the Main Stem Buffalo River and the headwaters of some of the larger southern tributaries: Little Buffalo River, Big Creek, and Cave Creek. Narrow valleys are typically found in the Everton Formation in the downstream reaches of the river and tributaries.

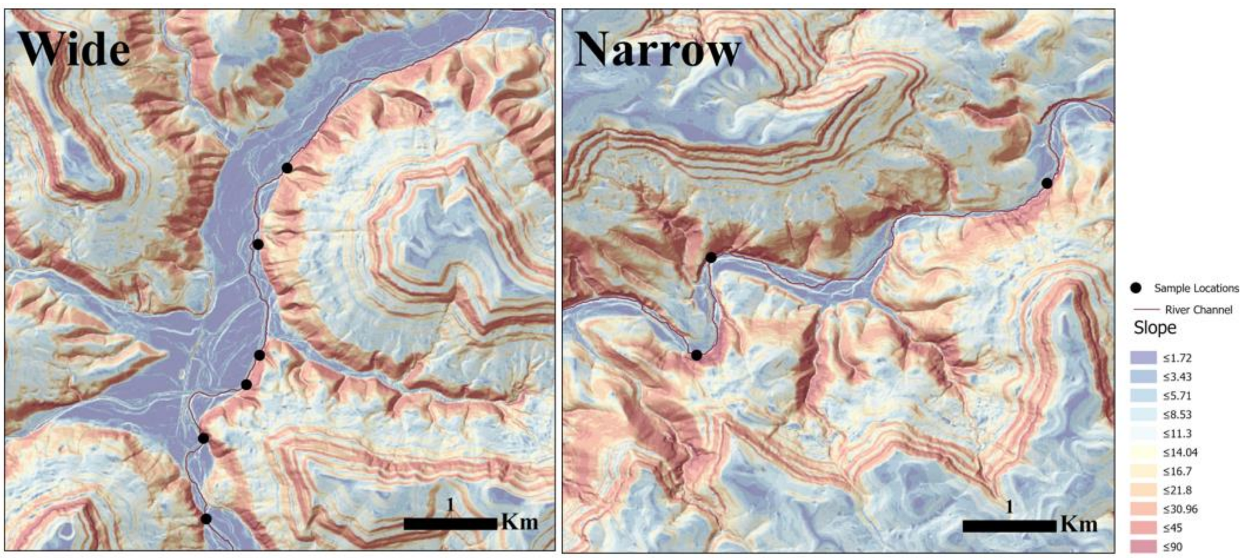

Figure 4: Digital elevation maps overlain with a slope layer for wide (left) and narrow (right) valleys in Buffalo River. This shows the difference between valley widths well as the valleys are flat in the color or blue. The wide valley (left) if found in the Boxley Valley area and the narrow valley (right) is found in the Ponca area downstream of Boxley Valley.

Within the study reaches there are two rock formations that make up the river valleys of interest: the Boone Formation and Everton Formation. The Boone Formation is a medium to thick bedded chert bearing limestone that is 95 to 115 m thick in the study area (Hudson & Turner, 2007). The Boone Formation is found in the upstream reaches of the study area; it is common to see karst topography in this formation. The Everton Formation is an interbedded sandstone, dolomite, and limestone sequence that is 95 to 110 m thick in the study area (Hudson & Murray, 2003). The Everton Formation contains the Newton Sandston Member, that often makes up prominent bluffs along the river (Hudson & Murray, 2003). The lithological transition from Boone to Everton is demarcated on the geologic map(s) as a red line (Figure 2). A distinct trend in valley narrowing is gradually observed downstream of the lithological transition. Previous studies have shown that Schmidt hammer values of the Boone and Everton Formations in the Buffalo River watershed were different than each other (Keen-Zebert et al., 2017; Thaler & Covington, 2016). Schmidt hammer values tell us about the rock's surface hardness, allowing us to compare rocks on a universal scale (Goudie, 2006; Thaler & Covington, 2016). Rock surface hardness is often used as a proxy for bedrock erodibility in field (Sklar & Dietrich, 2001). The Everton Formation Schmidt hammer values were lower than the Boone Formation meaning the Everton Formation has a lower erodibility.

Zunka (2018) found that there was a strong correlation between the migration rate of the river channel and the thickness of the rock exposed to active erosion especially in the massive Newton and St. Peter sandstones. Keen-Zebert et al. (2017) concluded that terraces found in the Buffalo River Valley were not a result of changes in climate, discharge, or base level change. Keen-Zebert et al. (2017) also found that changes in rock type of the modern floodplain were more important in determining whether strath terraces were preserved (Montgomery, 2004).

Thaler & Covington (2016), found that bedrock lithology did not control channel steepness in small tributaries on the Main Stem of the Buffalo River. Rather, channel steepness was controlled by the large blocks supplied to the river system from the massive sandstone unit that sit high in the stratigraphic column.

Chapter 4 - **Methods**

4.1 Site Selection

Site selection was an integral task in planning my field work at Buffalo National River. I used topographic, geologic, digital elevation maps, Google Earth cross sections, and preliminary scouting trips to choose data collection sites (Figure 2, 5). I marked many locations along various bluffs and steep areas along the river where we expected to find bedrock valley walls next to the channel. Sites were not set in stone; choices were refined as data collection continued (Figure 5).

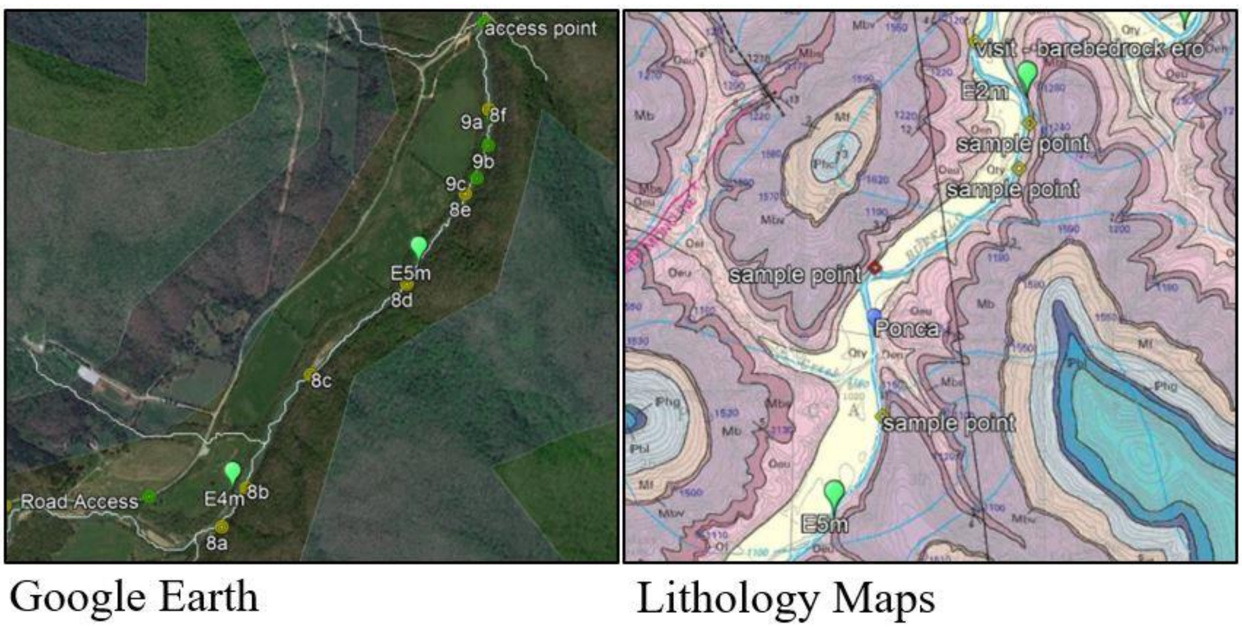

Figure 5: A map from Google Earth (left) and a lithology map (right) (Hudson & Murray, 2003) where I gathered cross sections to determine potential site locations. A good site had to have a bedrock valley wall directly next to the river channel.

A good site, according to my criteria, was a site with steep banks or bluffs with an exposed bedrock wall next to the channel. The maps clued me into whether the river was directly against the bedrock wall. I avoided locations that appeared to be near small drainages that join the Main Stem, landslides, or any other questionable non-talus bluff origin rock piles. Often, I believed that along full stretches good locations could exist and on those stretches I placed several pins (Figure 5). I chose representative sites along these reaches with several good possibilities. The goal was to provide a representation of the talus piles in each stretch. I used exploratory scouting trips to inform my decision-making processes for pre-field planning early in my research. Even with informed decisions, the on the ground knowledge was the most valuable to confirm the choices I made. The sites on the map, if they met our criteria, were used for field sampling. For example, if a potential site did not have talus at the base of the valley wall, but still met the criteria of an exposed bedrock wall next to the river channel, I still collected the other relevant measurements at this site. Sites with no talus were important for collecting a full data set. A lack of talus tells me that the river is actively moving talus blocks there, allowing the river access to the wall.

From the preliminary field work trip completed in January 2021, I estimated that approximately two to three sites could be visited and measured in a single day. This was a partial function of the difficulty in accessing locations, whether packing in or floating to the sites and the time it takes to collect measurements. There is private land on either side of some wide valley reaches specifically, forcing me to visit many of the wide valley sites by boat. In the end, I found that collecting about three sites was easily achievable in a day, and I could collect more sites per day as the field processes became more streamlined.

Approximately half of the data collection sites were in the wide bedrock river valleys and half were in the narrow bedrock river valleys on the Main Stem and the Little Buffalo. Twenty-six sites were measured on the Main Stem of the Buffalo River: ten in the Boone Formation and sixteen in the Everton Formation. Thirteen sites were measured on the Little Buffalo River, a large southern tributary of the Main Stem: seven locations in the Boone Formation, six in the Everton Formation. I ended with 40 sites total (Figure 2).

4.1.1 Brief Summary of Methods

In Buffalo River area, I measured grain sizes of talus blocks at the base of valley walls (Figure 6C, 6E), grain sizes of bedload (Figure 6D), bankfull width, and bluff wall height (Figure 6B) at my 40 site locations. I was interested in understanding the grain size distributions of talus and bedload as well as how frequently the different talus grain sizes could potentially move with different river discharges.

At each site, I made measurements and gathered notes and photographs. I noted our geographic location and talus pile dimensions (Figure 6A): length, width, and height. I took detailed notes on the physical condition of each site, included things such as: vegetation on the floodplain and talus pile, the location of gravel bars, visual descriptions of the bluff wall, talus and bedload grain descriptions. I also took pictures to document the site for visual reference (Figure 6).

Figure 6: (A) Talus at site E5m. The D50 grain size of talus is 341 mm, and the D84 talus grain size is 627 mm. The red line indicates the pile's extent, the yellow line indicates the height of the pile, the orange line indicates depth of the pile, and the blue line indicates length of the pile all within the extent of the picture. Note, this pile extends outside of the picture frame.

(B) Pictured is site E11m; mature trees and woody vegetation are within and scattered across the talus pile. In the background we can see the tall bedrock valley wall. The talus pile and the bedrock valley wall extend hundreds of meters along the river's edge. Long piles were common at many of the Everton Formation sites

(C) I am measuring large talus grains at E1m, an Everton Formation site location, using a measuring stick on the intermediate axis.

(D) Clay Robertson gathering bedload grain distribution data with a Wolman Pebble count at site E16m.

(E) Clay Robertson measuring talus grains at a Boone Formation site, B8m, using a measuring tape. These blocks are normally underwater; we knew the blocks were below water since we could see a stain line of where the water level usually is. This site was sampled in August of 2021, a time when water levels were low.

(F) Talus pile located at Jim Bluff, site E8m, a pile with little vegetation. The talus pile was sitting on top of a bedrock shelf under the bedrock wall's overhand. Clay is in the background and the kayak paddle is there for scale.

4.2 Grain Size Measurements

At each site, I measured grain sizes of the channel bed material and in the talus pile, if there was talus present. I measured grain size of the channel bedload on the gravel bar opposite or closest to the talus pile or we gathered from the riverbed near the talus pile when possible. The choice of location depended on the water level, temperature, and river morphology. The first option of using point bars was chosen as the temperatures were low and getting wet in cold conditions was unadvisable. The second option of gathering grain sizes within the channel could be safely done in late spring into the summer months with some gravel bars also measured in warmer months as well. At many locations the water was more than arm length deep, so we chose the gravel bars as sampling locations. I used the Wolman pebble count to characterize the bedload grain size (Figure 6D). At least 100 random grains were selected and measured with a standard gravelometer. How well sorted bedload material can be determined by the sorting coefficient, Equation 5 (Menting et al., 2015):

$$Sorting = \sqrt{\frac{D_{84}}{D_{16}}} \qquad \text{Equation 5}$$

I calculated how the bedload was sorted at each site location.

The talus grain size measurements were more involved. I created rules to determine how to make measurements that were appropriate and consistent between sites. Note, every sample location did not necessarily have a talus pile. For talus grain size measurements, we made a rule that assisted in determining where to begin and end the measurement of the talus pile. Sometimes the length of the talus pile had to be a judgement call, especially when the talus pile extended down an extensive section of the bluff wall, generally more than 50 meters. The section that was representative of the pile was chosen as the location at which we took talus grain size measurements. For long piles, often found in the Everton Formation, I stretched a tape measure approximately 30 m parallel to the bluff face both at third and two thirds up the talus pile, depending upon the talus pile characteristics. Two or more shorter lines perpendicular to the bluff wall were also made, creating a grid type pattern to collect data on talus sizes along the slope when more grains were needed for a sample. Talus pile shape varies greatly, so the lines varied to get the best representation of the talus grain in the pile that was possible (Figure 6E). Along these lines every meter or half meter talus grain sizes were measured. Every half meter was used universally unless there were talus blocks at the site that were one meter or greater in diameter. We would use the interval of one meter for these piles. I used a measuring tape to measure the b-axis (Figure 6C). The b-axis is the intermediate axis of the block; it is perpendicular to the longest axis of the block (Verdian et al., 2020). Blocks that appeared to be rounded, imbricated, or otherwise suspected of being transported by the river were not measured; this was done to make sure only collapsed material from the bedrock wall was measured. For each block I noted the lithology, either sandstone or limestone.

The number of talus grains measured at each location was often limited to the number of blocks present for measurement. We would choose to measure more, but at several locations there were only a few talus blocks present for measurement. Fifty blocks were chosen as an approximate adequate number of blocks. Our methodology was about getting a representative sample, if there were fewer than approximately 50 talus blocks present, I measured all blocks at the location. The bigger the blocks, the more measurements that are needed. At some locations, multiple smaller piles make up a larger site sample. I created rules to collect talus grains if there were sub-populations of grains amongst the larger sets indicating that there may be different depositional time frames. I took detailed notes about the separate talus cones or piles that were along a stretch I had marked out. In this way, this indicates that these populations are from different fall events and may have a different age.

Talus pile characterization also included measuring the pile dimensions. I used a Laser Technology Inc. TruPulse 200x laser range finder to take large-scale measurements like talus pile dimensions (Figure 6A). The laser range finder is accurate to the centimeter, easy to transport, and reliable for measurement taking. In the field, standing across from the talus pile I used a laser range finder to measure three critical components to estimating volume of the pile. I measured vertical distance, horizontal distance, and incline.

4.3 Other Field Measurements

I used the TruPulse 200x laser range finder to measure bluff height. I sat on the ground to measure the height of the bedrock valley wall that the talus fell from. I measured from the base of the talus pile to the top of the bedrock valley wall when vegetation was not obscuring the view. If vegetation was an issue, I moved in the horizontal direction to see if some bluff face was exposed, using that as a proxy for the bluff height for the location of the pile.

Along with the grain size distribution data, I characterized all sites and basic channel measurements in the wide and the narrow valleys. I measured bankfull width for each location using the laser range finder to measure a horizontal distance, on a level field, determined to be the bankfull width. I determined width by using the base of the perennial vegetation along with indicator marks that helped determine if water was present there for a period of time, usually characteristic of an annual or two-year flood. I took notes on observed high-water marks above the bankfull width. High water marks are important because they can tell us the height of flow the river may expect above normal bankfull suggesting that a recent high flow event may have occurred. These markers can be anything from piles of sand or leaves and branches that look like they had been collected high up in branches during high flow. They could also be something as simple as water marks on tree trunks or rocks. With that, I hoped to potentially capture the height of water, but since branches sometimes bend in large events, I concede that those high water marks could be deceiving. Lastly, I took notes and pictures of talus piles, bedload, vegetation, and the site location to make determining things like the roughness factor easier to estimate once field work was completed.

Digital elevation maps provided a key component to fill in data that we could not gather by hand or get from outside sources. We used 9-meter DEMs (USGS, 2022) of the study area to extract drainage area and slope. We gathered measurements of slope, using a smoothed stream profile from a DEM. Since we had only four river discharge stations along the Main Stem of the river, we could not use those discharge values as accurate values for each location. In Figure 7, the peak discharges per USGS gauge is recorded for reference. To get to site specific discharge I used DEM derived drainage areas to calculate a discharge value for each site.

4.4 Discharge Calculations

In order to find the magnitude of the 2-year, 100-year, and 1,000-year flood discharge at each sample location, I used the Frequency Curve Version 3.06 spreadsheet released in August

2014 by the National Resource Conservation Services; I created flood frequency curves (Moore, 2014). Frequency curves show the probability of various event sizes at each of the four gauge locations in our area of interest, Boxley, Ponca, Pruitt and St. Joe, occurring in a given year by observing the discharge and year in respect to the curve (Figure 8). This intersection gives the probability of an event of a certain magnitude. With the data from the NRCS flood frequency curves we took the discharges from the four gauge stations for the 2-year, 100-year, and 1,000-year floods. The longest USGS discharge gauge record showed data for 50 years. Using the discharge from the gauge against plotted against the drainage area at the discharge gauge, we fit a straight line (Figure 9). The equation derived from the fitted data allowed us to calculate discharge at each site location (Figure 9).

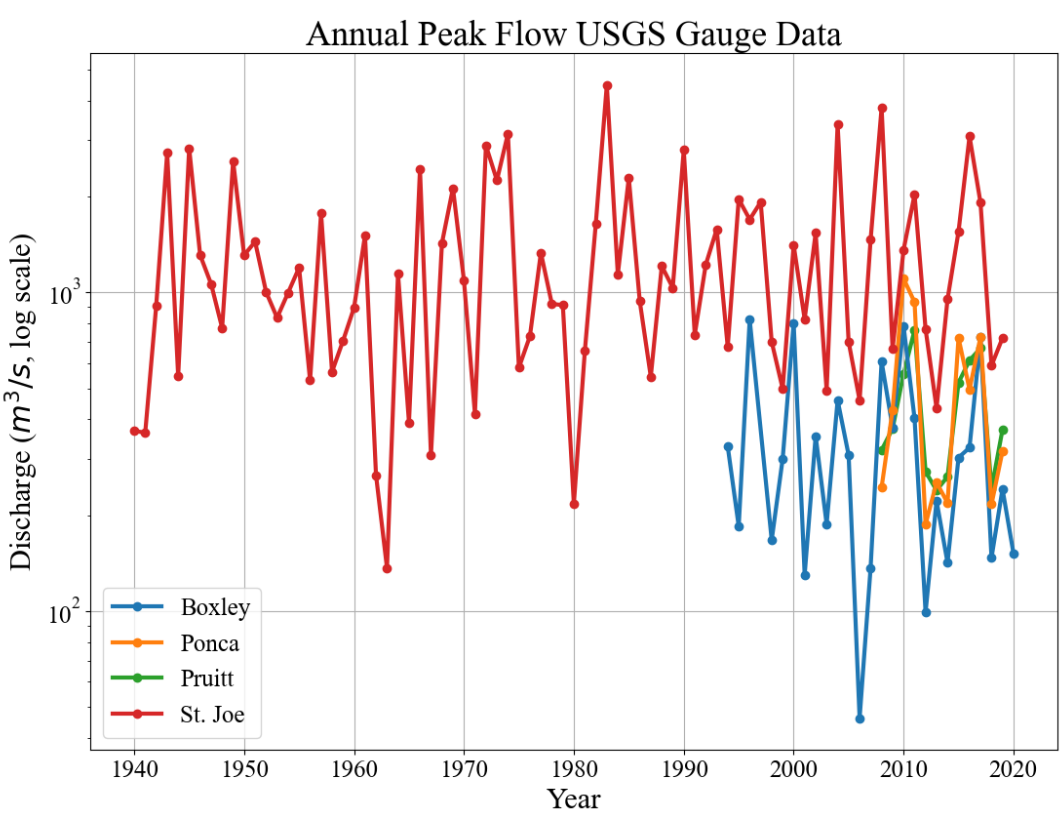

Figure 7: Peak flow events for the Boxley, Ponca, Pruitt, and St. Joe discharge gauges (USGS, 2022) from 1940 to 2020. On the y-axis is discharge in m^3/s (log scale) and on the x-axis is time in years.

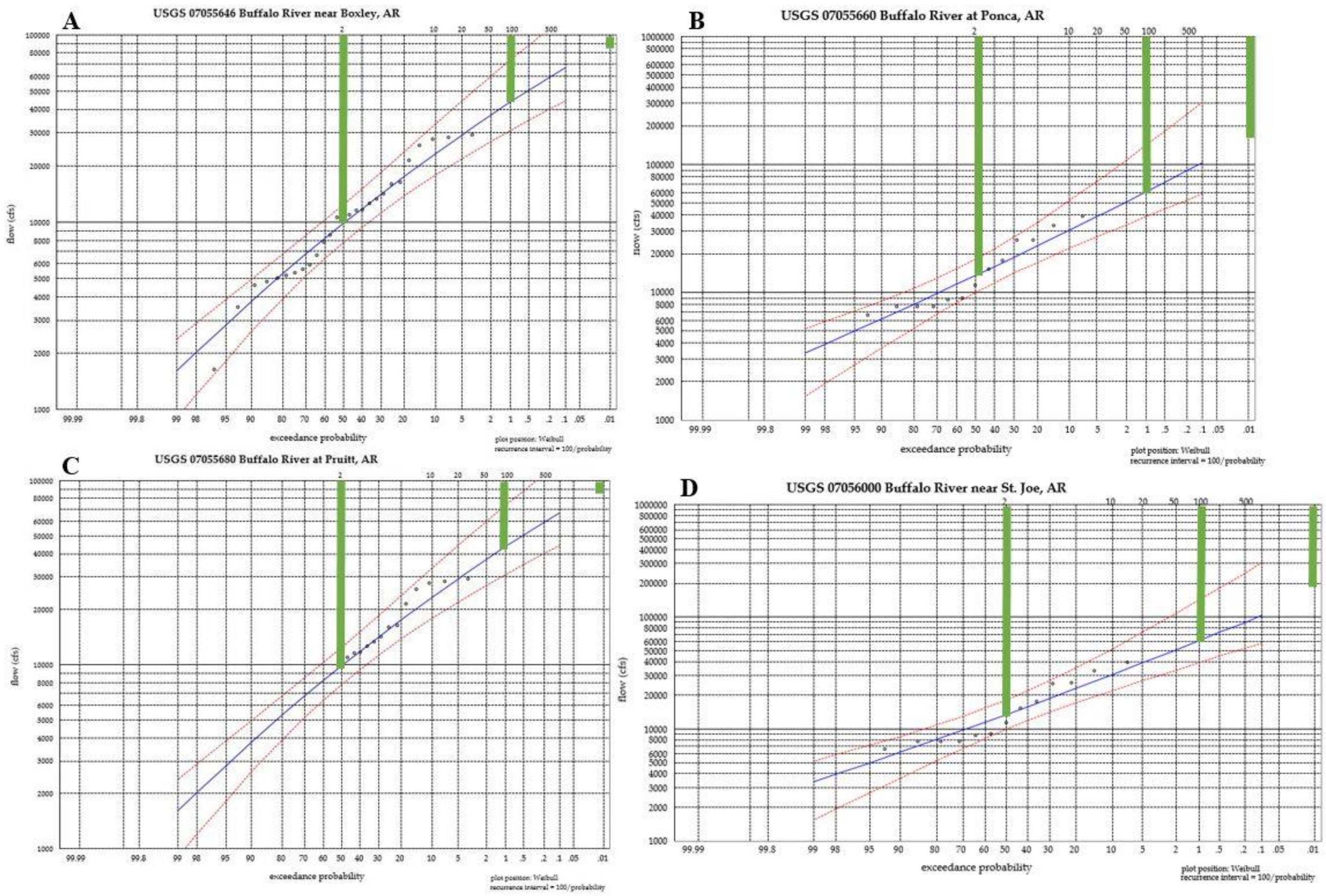

Figure 8: Flow frequency curves for the Boxley, Ponca, Pruitt, and St. Joe gauges provided by the NRCS spreadsheet (Moore, 2014). The ability to project the probability of a certain size event depends on the amount of input data available. On the y-axis is discharge (cfs) and on the x-axis is exceedance probability as a percentage. The blue line is a trend line with two red curved lines on either side showing the possible deviation from the blue trend line. I have added three vertical, green lines per graph to indicate the discharge predicted for the 2-year, 100-year, and

1,000-year flood events. In Table 1 the maximum discharge and 2-year flood from each gauge is listed per USGS gauge.

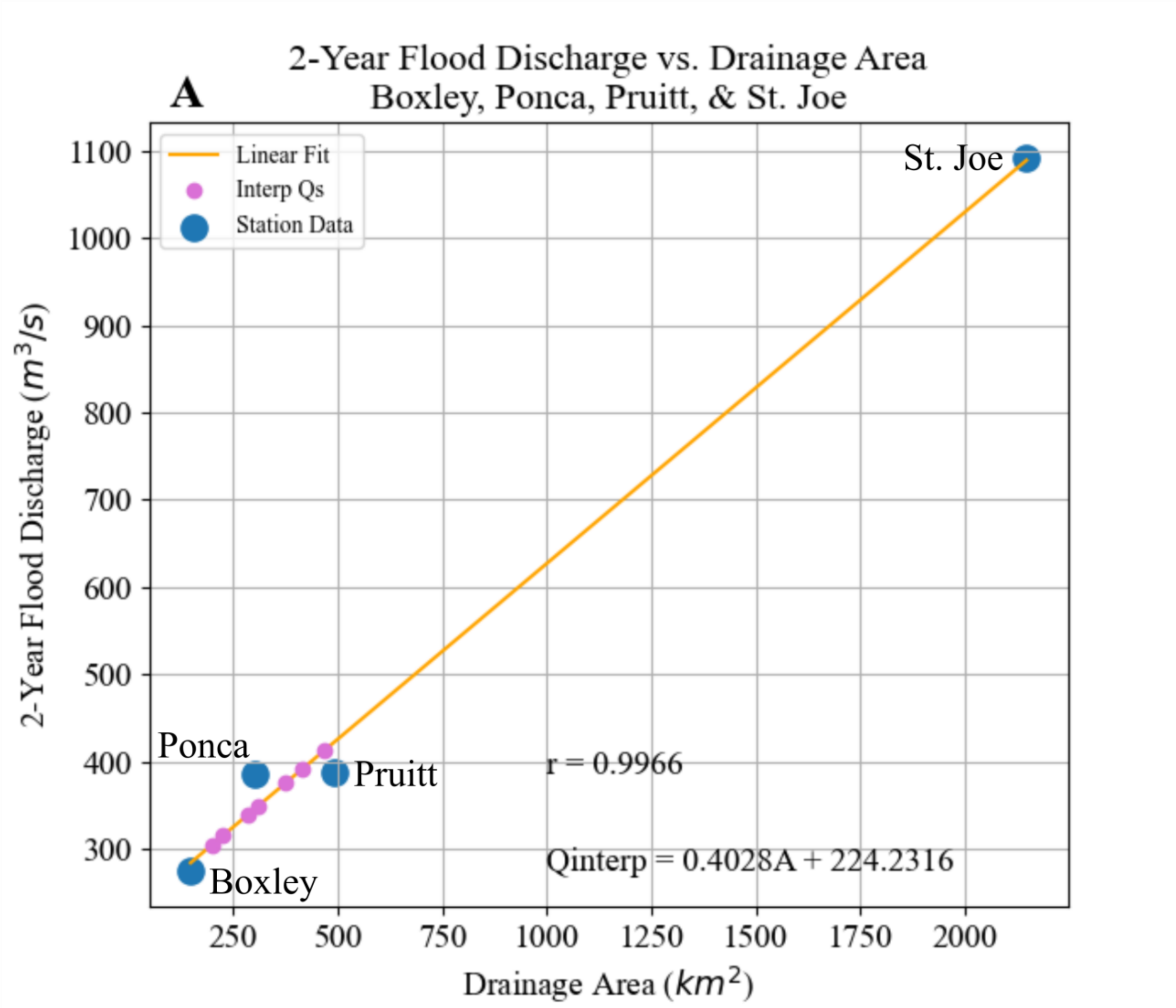
A
2-Year Flood Discharge vs. Drainage Area
Boxley, Ponca, Pruitt, & St. Joe
Linear Fit
Interp Qs
Station Data
St. Joe
Ponca
Pruitt
Boxley
r = 0.9966
Qinterp = 0.4028A + 224.2316
2-Year Flood Discharge (m^3/s)
Drainage Area (km^2)
1100
1000
900
800
700
600
500
400
300
250
500
750
1000
1250
1500
1750
2000

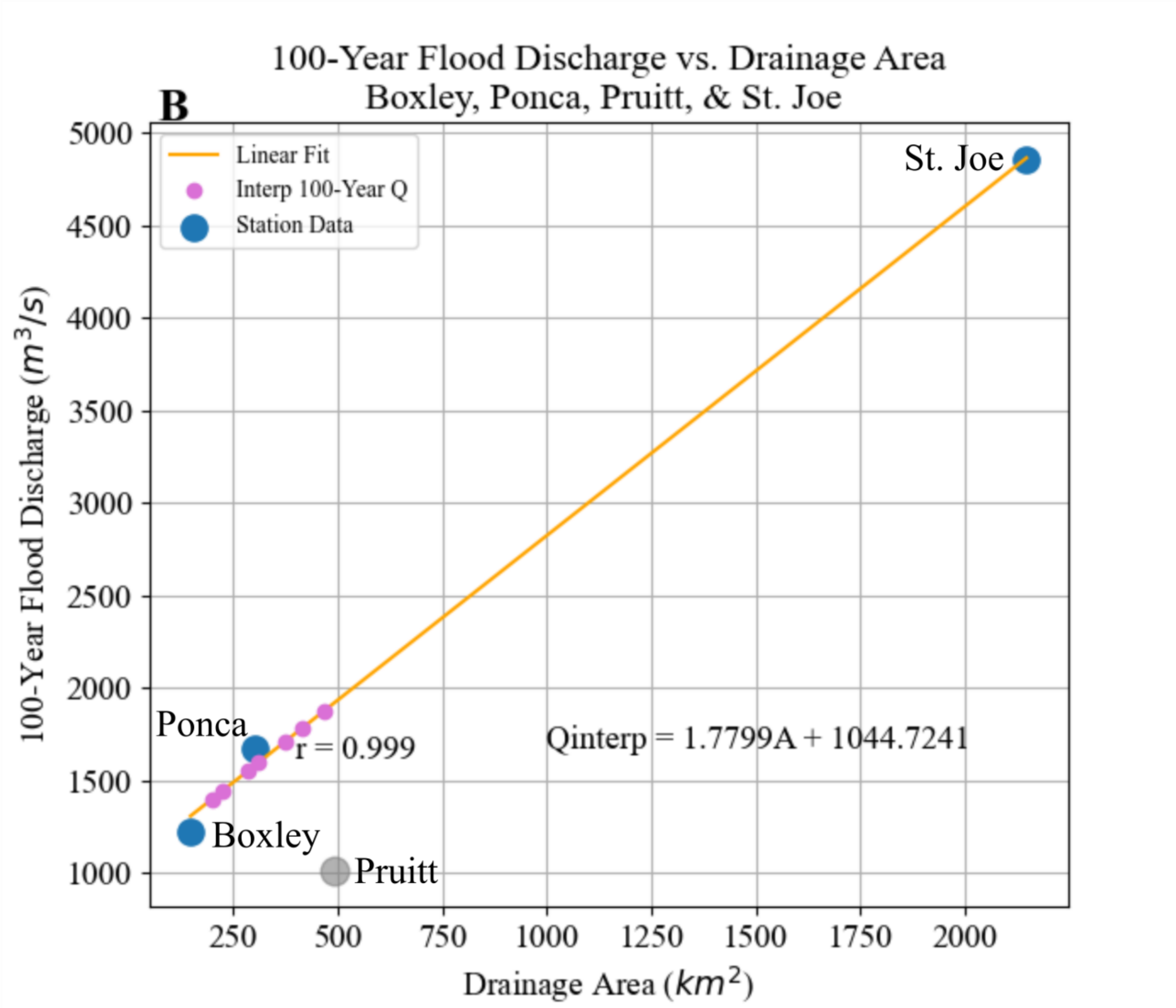
100-Year Flood Discharge vs. Drainage Area
Boxley, Ponca, Pruitt, & St. Joe
B
Linear Fit
Interp 100-Year Q
Station Data
St. Joe
Ponca
r = 0.999
Qinterp = 1.7799A + 1044.7241
Boxley
Pruitt
100-Year Flood Discharge (m^3/s)
Drainage Area (km^2)
5000
4500
4000
3500
3000
2500
2000
1500
1000
250
500
750
1000
1250
1500
1750
2000

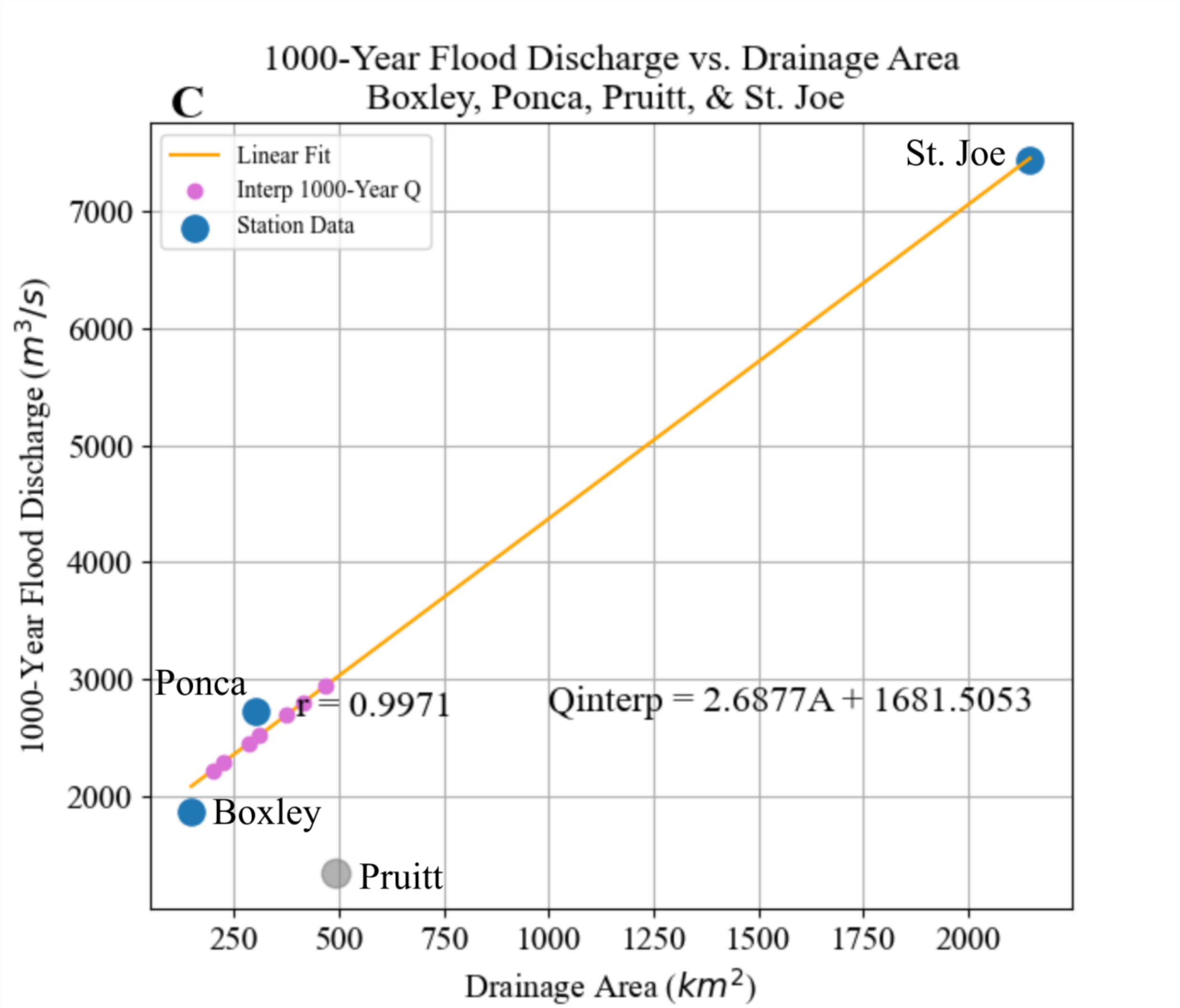

Figure 9: (A) Boxley, Ponca, Pruitt, and St. Joe river gauge discharge (m^3/s) data, y-axis, for the 2-year flood plotted against drainage area (km^2), x-axis. From the data I fitted a line to derive an equation with which discharge could be calculated at each of our site locations on the Buffalo River.

(B) Boxley, Ponca, and St. Joe river gauge discharge (m^3/s) data, y-axis, for the 100-year flood plotted against drainage area (km^2), x-axis. From the data I fitted a line to derive an equation with which discharge could be calculated at each of our site locations on Buffalo River. Note, the Pruitt gauge is the greyed out circle on this graph; there is not enough data to get an accurate value for this discharge. At times, Pruitt had discharge values that were lower than the upstream Ponca gauge.

(C) Boxley, Ponca, and St. Joe river gauge discharge (m^3/s) data, y-axis, for the 1,000-year flood plotted against drainage area (km^2), x-axis. From the data I fitted a line to derive an equation with which discharge could be calculated at each of our site locations on Buffalo River. Note, the Pruitt gauge is the greyed out circle on this graph; there is not enough data to get an accurate value for this discharge. At times, Pruitt had discharge values that were lower than the upstream Ponca gauge.

4.5 Shear Stress Calculations

I calculated shear stress exerted by the river during a 2-year, 100-year, and 1,000-year flood using Equation 6.

$$\tau_b = \rho g \frac{nQ}{w}^{3/5} S^{7/10} \qquad \text{Equation 6}$$

τ_b is the basal shear stress, ρ is the density of water, g is gravity, *w* is the measured river bankfull channel width, *n* is Manning's roughness coefficient, estimated from charts to be 0.04 for my calculations, *Q* is discharge, and *S* is the slope of each site, measured using a DEM.

Knowing the shear stresses needed to potentially move different block sizes allowed me to calculate the size block that the river can potentially move during bankfull and peak flow events. The critical shear stress is the shear stress produced by the river discharge needed to potentially move a block of a certain size for both the talus and the bedload grains (Equation 4). I calculated critical shear stresses for the D84 and D50 grain sizes of both the bedload and talus grain size distributions. With this critical shear stress, I determined the size discharge event needed to move the blocks at that specific river valley location (Equation 6) (Snyder et al., 2003).

Using these shear stress calculations, I used an excess shear stress ratio: basal shear stress divided by critical shear stress. I did this for various combinations of grain sizes and flood sizes of interest, D50 and D84 grain sizes and 2-year, 100-year, and 1,000-year floods. When excess shear stress values are below one, talus grains have no potential for movement. If the values are above one there is a potential for talus grain movement.

Chapter 5 - **Results**

Of the 40 site locations, 26 sites were on the main stem of Buffalo National River, 10 in the Boone Formation, and 16 in the Everton Formation. In the tributaries there were 14 sites total, 7 in the Boone Formation on the Little Buffalo River, 6 in the Everton Formation on the Little Buffalo River, and 1 on Big Creek in the Boone Formation. While some narrow valleys do occur in the Boone Formation and wide valleys occur on a short reach of the Everton Formation in this study most wide valley locations occurred in the Boone Formation and all narrow valley locations occurred in the Everton Formation.

5.1 Basic Measurements Results

5.1.1 Drainage Area, Slope, and Channel Width

We extracted the drainage areas and slopes from digital elevation maps and measured the bankfull width in the field for each site location (Table 2). These were necessary pieces of data to collect to calculate discharge for each site as well as the calculation of shear stress since slope and channel width are explicitly within our basal shear stress calculation (Equation 6).

Going upstream to downstream on the Main Stem and in the Little Buffalo the graph and table (Figure 10A 10B, Table 2) show that the river increases in drainage area in the downstream direction, usually with some significant jumps. The confluence of the Little Buffalo with the Main Stem Buffalo River occurs after E17m. The drainage area of E17m is 482 km^2. The addition of tributaries normally increases the drainage area in most river systems which then increases the calculated discharge based on the added drainage area.

Slope generally decreases in the downstream direction in our field sites, which is expected although, depending on the length of reach used for measurement the slope can be a more localized measurement (Figure 10C, 10D). We generally expect there to be an increase in channel width in the downstream direction. Channel width does increase going in the downstream direction of the Little Buffalo River (Figure 10F), but that trend is less well defined in the Main Stem Buffalo River (Figure 10E). Downstream of site E7m channel width ranged from 50 to 55 m at the widest to 20 to 35 m at several locations with some substantial channel narrowing at some downstream sites, there appears to be a trend of increasing channel width going downstream.

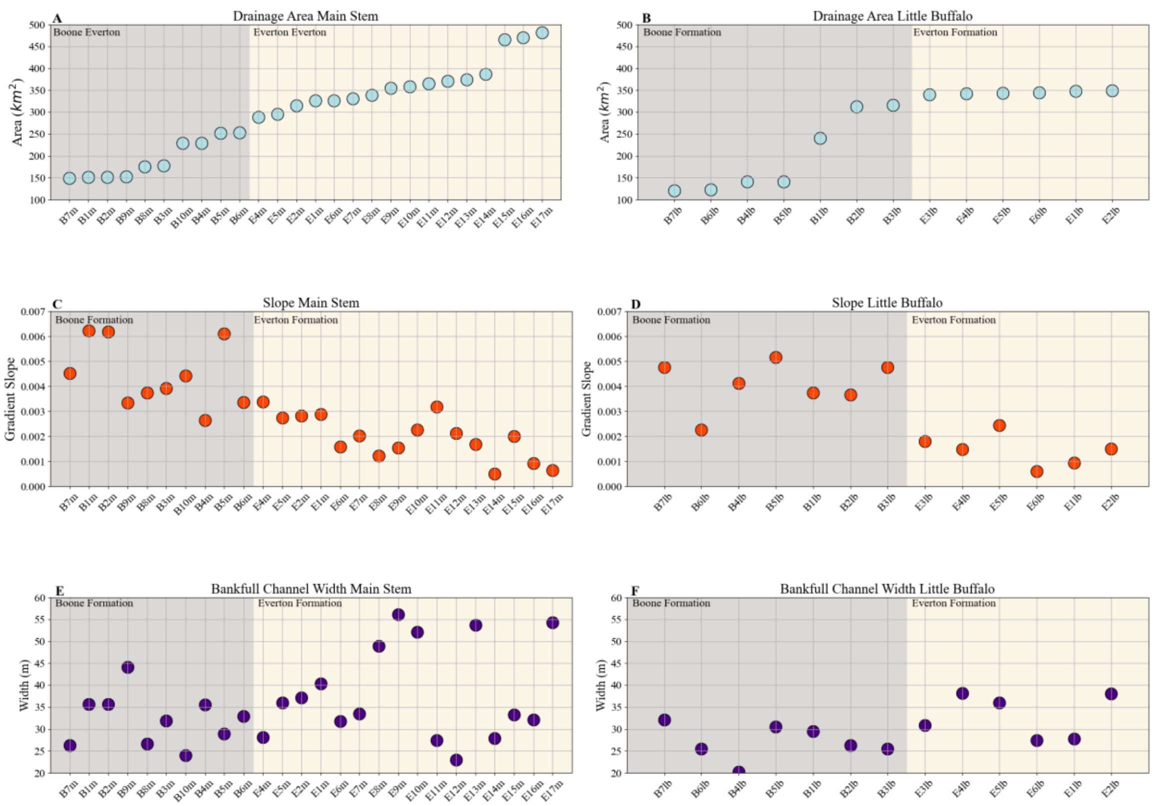

Figure 10: (A) Drainage area (km^2) on the y-axis with Main Stem site locations in the upstream to downstream order on the x-axis (unitless).

(B) Drainage area (km^2) on the y-axis with Little Buffalo site locations in the upstream to downstream order on the x-axis (unitless).

(C) Degree slope on the y-axis with Main Stem site locations in the upstream to downstream order on the x-axis (unitless).

(D) Degree slope on the y-axis with Little Buffalo site locations in the upstream to downstream order on the x-axis (unitless).

(E) Bankfull channel width (m) on the y-axis with Main Stem site locations in the upstream to downstream order on the x-axis (unitless).

(F) Bankfull channel width (m) on the y-axis with Little Buffalo site locations in the upstream to downstream order on the x-axis (unitless).

Table 2: Measured field data (channel width and grain sizes for talus and bedload) and DEM data (slope and drainage area) per site location of the Main Stem Buffalo River and Little Buffalo River going from the most upstream site location to the furthest downstream.

Site	Slope	Drainage Area (km^2)	Channel Width (m)	D50 Talus (mm)	D84 Talus (mm)	D50 Bedload (mm)	D84 Bedload (mm)
B7m	0.0045	149	26.3	376	942	140	303
B1m	0.0062	152	35.7	223	426	34	71
B2m	0.0062	152	35.7	97	200	38	64
B9m	0.0033	153	44.2	609	867	42	116
B8m	0.0037	176	26.6	288	476	89	168
B3m	0.0039	178	31.9	238	491	26	41
B10m	0.0044	229	24.0	286	554	112	176
B4m	0.0026	229	35.5	174	321	53	133
B5m	0.0061	252	28.9	NA	NA	84	140
B6m	0.0034	253	32.9	447	1013	57	113
E4m	0.0034	289	28.1	418	932	57	120
E5m	0.0027	295	36.0	341	627	84	153
E2m	0.0028	315	37.1	367	822	58	109
E1m	0.0029	326	40.4	318	674	45	85
E6m	0.0016	327	31.7	342	761	33	69
E7m	0.0020	331	33.5	325	506	43	88
E8m	0.0012	339	49.0	342	653	27	47
E9m	0.0015	355	56.2	NA	NA	52	100
E10m	0.0023	358	52.1	395	635	46	89
E11m	0.0032	365	27.5	311	674	77	124
E12m	0.0021	371	23.0	263	427	52	99

E13m	0.0017	374	53.8	346	1080	33	74
E14m	0.0005	387	27.9	417	669	27	48
E15m	0.0020	466	33.3	436	696	38	70
E16m	0.0009	470	32.1	431	832	55	94
E17m	0.0006	482	54.3	542	781	36	62

Little	Buffalo	River					
Site	Slope	Drainage Area (km^2)	Channel Width (m)	D50 Talus (mm)	D84 Talus (mm)	D50 Bedload (mm)	D84 Bedload (mm)
B7lb	0.0048	121	32.1	293	507	48	100
B6lb	0.0023	122	25.5	NA	NA	83	160
B4lb	0.0041	141	20.2	483	822	84	153
B5lb	0.0052	142	30.5	NA	NA	91	165
B1lb	0.0037	241	29.5	NA	NA	35	76
B2lb	0.0037	313	26.3	NA	NA	33	71
B3lb	0.0048	317	25.5	319	715	41	73
E3lb	0.0018	339	30.9	416	659	57	104
E4lb	0.0015	343	38.2	334	725	31	68
E5lb	0.0024	343	36.0	410	955	62	99
E6lb	0.0006	344	27.4	486	953	55	109
E1lb	0.0009	348	27.8	261	407	48	83
E2lb	0.0015	349	38.1	502	1013	46	85

5.1.2 Qualitative Description of Talus Piles

Talus grain sizes vary to a great extent between the two valley types, wide and narrow. The piles, visually, were all very different. Sites had piles that ranged anywhere from a small number of blocks sitting on a bedrock ledge (Figure 6F) to a full cone-shaped pile with many grains (Figure 6A, 6E). Some piles extend well into the channel where I saw blocks under water while others sat on bedrock ledges away from the water. I floated by blocks that themselves were larger in size than vehicles and provide scale for how enormous talus blocks could be for a river to transport.

In the Everton Formation, I noticed that I often found piles stretching along lengths of the valley wall, some 300 to 400 meters long. In the Boone Formation, I saw something very different, long stretches were not as common. Specifically, in the Boone Formation, the wide valleys, more locations completely lacked talus piles all together. In the Everton Formation, sites without talus were less common.

Piles almost always had vegetation covering them to some extent, many with large, mature trees growing amongst the blocks. The more mature vegetation (~ 7 cm in diameter) was commonly present at both the wide and narrow valleys (Figure 6B). I did find some sites with little to no vegetation on the piles (Figure 6F). Blocks, particularly in the narrow valleys, had moss covering the blocks making the determinations of lithology much more challenging; in these places we generally found mature vegetation.

5.1.3 Grain Size Distributions

Bedload

Bedload grain size generally decreases in size, in a downstream direction (Figure 11). There is a substantial decrease in bedload grain sizes going downstream by looking at the D50 grain size for both the Main Stem River and the Little Buffalo River (Figure 11).

The D50 for the Main Stem Buffalo River bedload was typically around 65 mm and decreases to about 40 mm in the downstream reaches (Table 2). In the Little Buffalo River, bedload D50 grain sizes range from around 60 mm at the most upstream sites to 30 to 50 mm in the downstream sites (Figure 11). Grain size values vary quite a bit between the upstream and downstream sections of the sites.

Sorting coefficients (Equation 5) for bedload ranged from 1.64 to 3.23. The well sorted bedload grain distributions are closer to the 1.64 values while the poorly sorted are closer to the 3.23 value. Within our data the mean amongst all sites is 2.07. The Main Stem's bedload grain sorting values decrease going downstream. That decreasing trend was not apparent in the Little Buffalo.

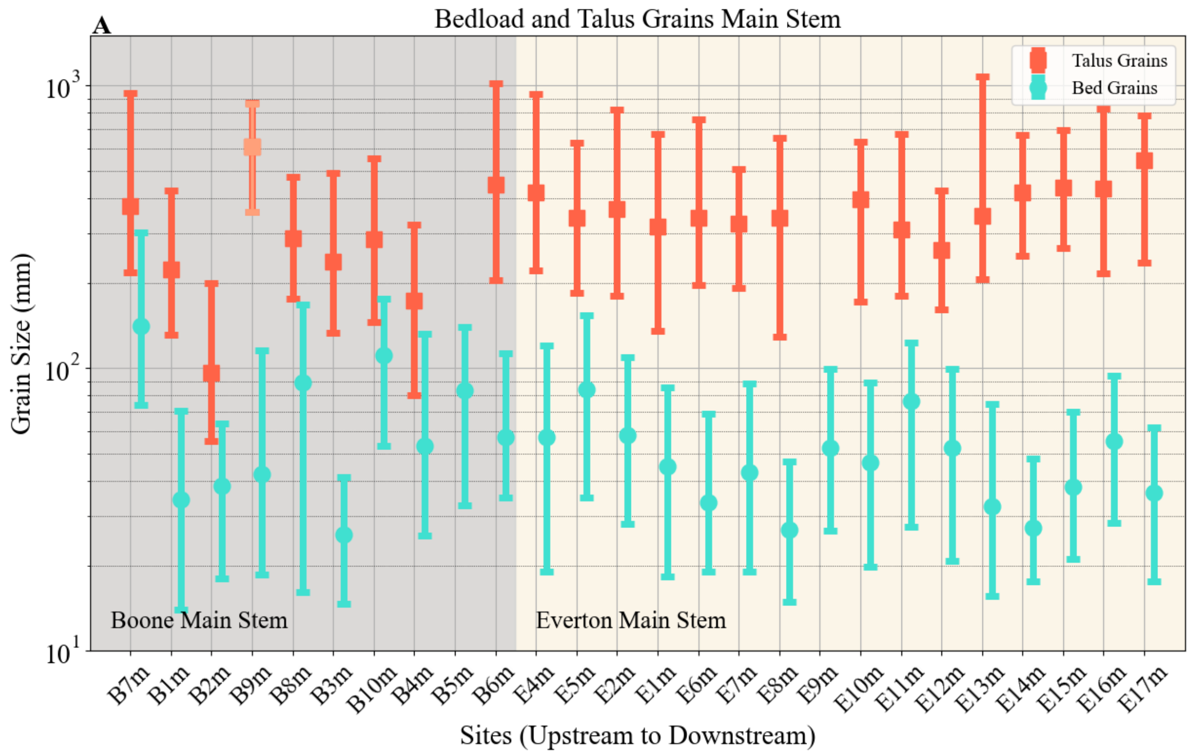

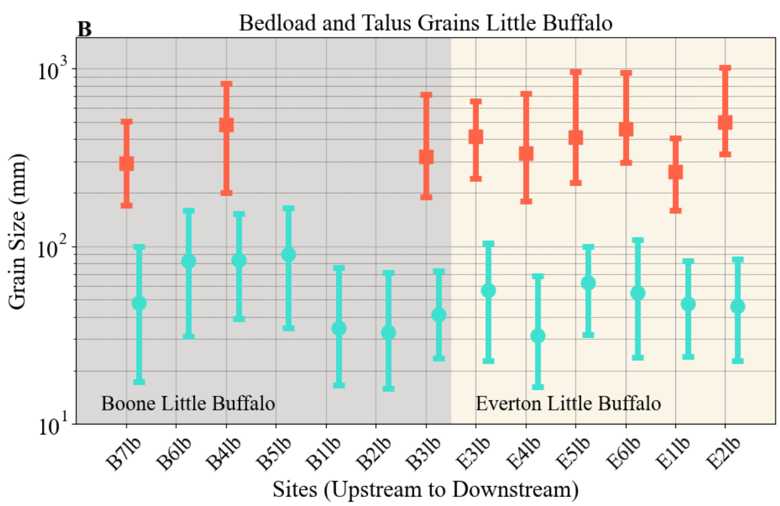

Figure 11: (A) All site locations on the Main Stem of the Buffalo River in the upstream to downstream order on the x-axis (unitless). Grain size (mm) is on the y-axis on a log scale. The bedload distributions are in orange with the partnering talus distribution in teal. The top whisker is the D84 grain size, the circle or square is the D50 grain size, and the bottom whisker is the

D16 grain size. Boone Formation is in the upstream reaches, shown in as a grey box while the Everton Formation is in the downstream reaches, shown as a tan box. The light orange talus bar at site B9m has only six blocks making up the talus block distribution. We exclude B9m as a talus pile with a reliable sample size for analysis.

(B) All site locations on the Little Buffalo River in the upstream to downstream order on the x-axis (unitless). Grain size (mm) is on the y-axis in log scale. The bedload distributions are in orange with partnering talus distributions in teal. The top whisker is the D84 grain size, the circle or square is the D50 grain size, and the bottom whisker is the D16 grain size. Boone Formation is in the upstream reaches, shown in as a grey box while the Everton Formation is in the downstream reaches, shown as a tan box.

Talus

The grain size distribution and cumulative frequency curves of the Boone and Everton Formations (Figure 11, 12, 13) display how the talus grain populations relate to each other. Using statistical t-tests, we tested whether the means of the cumulative lithologies per river stretch in both Main Stem and Little Buffalo, to see if the Boone Formation was different from the Everton Formation. We used a level of significance of $p < 0.05$. Talus grains in the Main Stem Boone Formation were substantially and significantly smaller than the Everton Formation (D50 = 244 mm Boone Formation versus D50 = 349 mm Everton Formation; $p = 0$). Talus grains in the Little Buffalo Boone Formation were substantially and significantly smaller than the Everton Formation (D50 = 314 mm Boone Formation versus D50 = 386 mm Everton Formation; $p = 0.0075$).

We found significant and substantial differences in talus grain size between the Boone Formation and the Everton Formation in both the Main Stem Buffalo River and the Little

Buffalo River. The Everton Formation of the Main Stem and Little Buffalo were statistically the same where the Boone Formation of the two were statistically different.

Boone Formation talus grain sizes were smaller overall and had a larger range of sizes compared to the Everton Formation (Figure 11). If I combine all Boone Formation Main Stem sites into one distribution (Figure 12A), the D50 is 244 mm. For the Everton Formation Main Stem, the combined D50 is 349 mm (Figure 12B). The range for the Boone Formation talus grain D50 sizes is much larger than I see in the Everton Formation (about a 233 mm larger range than in the Everton Formation). The Boone Formation range is greater than the Everton Formation talus grain range. D50 grain size ranges from 97 mm to 609 mm in the Boone Formation versus 263 mm to 542 mm in the Everton Formation. The blocks of the Everton Formation talus are generally larger than the Boone Formation talus even though the Boone Formation in the Main Stem has a large range of talus block sizes. Some of the largest blocks in the Boone Formation are around 1,021 mm, while talus blocks in the Everton are about 1,080 mm. The combined cumulative frequency curves show Everton sites have larger grains than the Boone sites (Figure 13).

The Boone Formation in the Little Buffalo also has smaller grains than the Everton Formation. The D50 of the Boone Formation in the Little Buffalo is 314 mm while the D50 of the Everton Formation is 386 mm (Figure 12A, 12B). The Boone Formation's range in the Little Buffalo is narrower than that of the Everton Formation (293 mm to 483 mm versus 261 mm to 502 mm, Figure 12).

Using the cumulative frequency curve for each lithology, we compare the tributary, Little Buffalo, to the Main Stem Buffalo River (Figure 13). The cumulative Main Stem D50 Boone Formation is 244 mm while the Little Buffalo's is higher at 314 mm. In the Everton Formation sites the D50 in Little Buffalo is 386 mm while the Main Stem Everton is slightly lower at 349 mm. In both lithologies the Little Buffalo had consistently higher values for the fewer samples there. Talus grains in the Main Stem Boone Formation and talus grains in the Little Buffalo Boone Formation were statistically different (D50 = 417 mm Main Stem Boone Formation versus D50 = 429 mm Little Buffalo Boone Formation; $p = 0.0145$). Talus grains in the Main Stem Everton Formation and talus grains in the Little Buffalo Everton Formation were statistically the same (D50 = 551 mm Main Stem Everton Formation versus D50 = 615 mm Little Buffalo Everton Formation; $p = 0.0665$). Keep in mind that the Little Buffalo had fewer sites that comprised the cumulative grain frequency curve (Figure 13). The Boone Formation grains in both the Main Stem and the Little Buffalo are smaller than those of the Everton Formation Main Stem and Little Buffalo. The Little Buffalo appears to have larger grains than the Main Stem when observing the cumulative frequency curves (Figure 13).

5.1.4 Bedload and Talus Together

The bedload and talus grains in the Boone Formation, wide valleys, sometimes overlap and are much closer to each other than the talus and bedload grains in the Everton Formation, narrow valleys, per site location. In the downstream direction, into the Everton Formation, narrow valleys, a separation between bedload and talus forms, where I observe an ever-increasing gap between the distributions in the downstream direction (Figure 11).

Comparing talus and bedload grain sizes at each site may hint at a relationship that could tell about potential talus movement. In the Main Stem Boone Formation, five sites have an overlap between the D84 bedload grain and the D16 talus (Figure 11). For example, site B7m, the D84 bedload is 85 mm larger than the D16 talus. The overlap in grain sizes in talus and bedload tell that bedload grain sizes are regularly transported that are larger than blocks in the talus piles. We do not see this overlap in talus and bedload grain size in the Main Stem Everton Formation. Sites E5m was the closest site in the Everton Formation to having overlap in between the bedload and talus grain sizes. At E5m, the D16 talus was 32 mm larger than the D84 bedload. At most other Everton Formation sites D16 talus are ~115 mm larger than the D84 bedload.

In the Little Buffalo Boone Formation, only three of the six sites had talus grains. There were no locations where the D84 bedload and the D16 talus grains overlapped, but the grain sizes were much closer to each other than the sites in the Little Buffalo Everton Formation. For example, the D16 talus was only 43 mm larger than the D84 bedload at site B4lb and 76 mm larger at E1lb. The difference between the D16 talus and D84 bedload in the Boone formation is smaller (43 mm) compared to the difference we saw in the Everton Formation (76 mm).

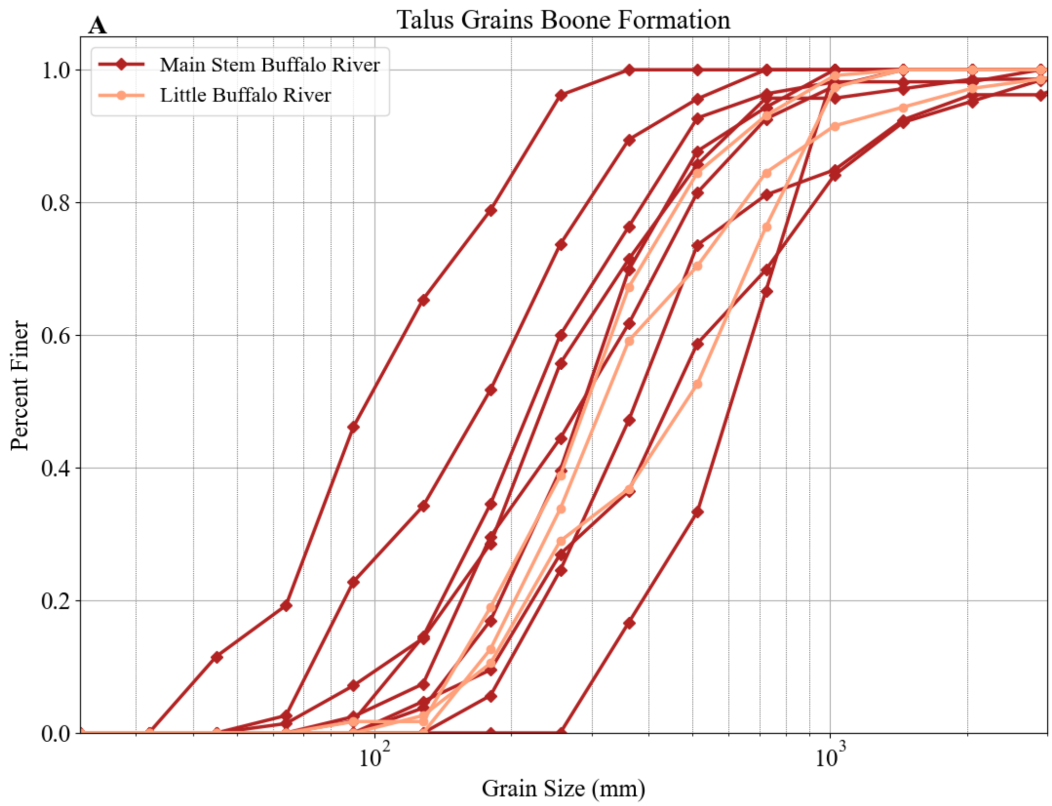
A
Talus Grains Boone Formation
Main Stem Buffalo River
Little Buffalo River
Percent Finer
0.0
0.2
0.4
0.6
0.8
1.0
10^2
10^3
Grain Size (mm)

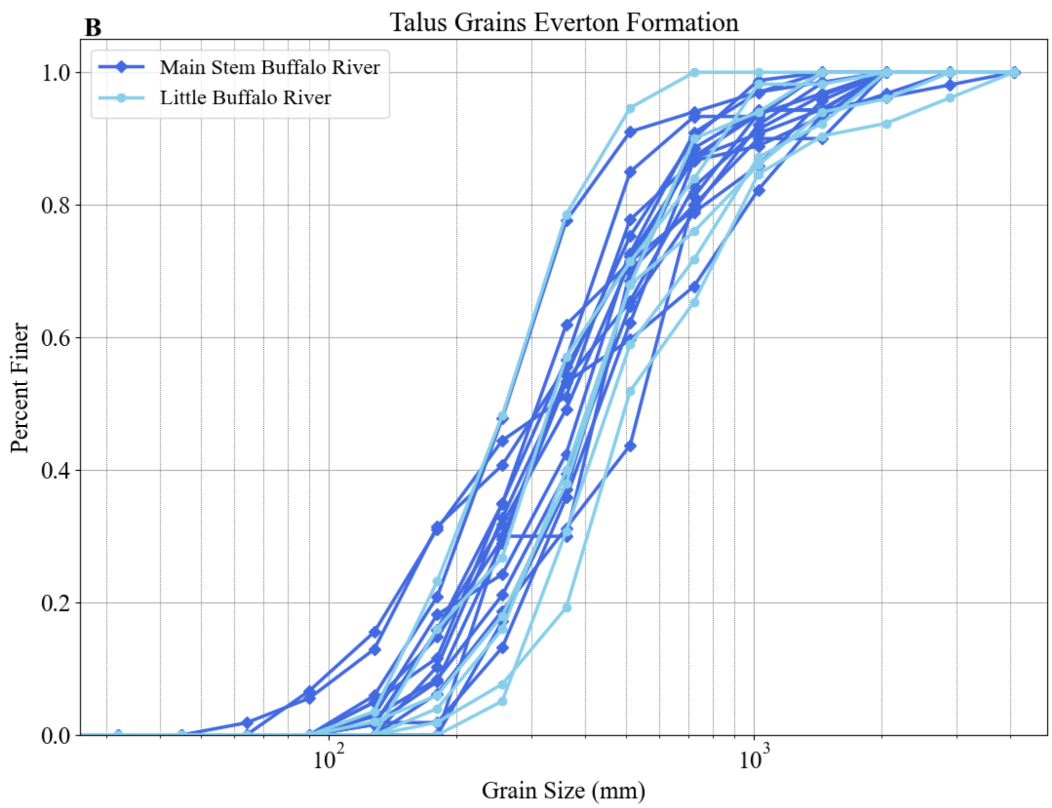
B
Talus Grains Everton Formation
Main Stem Buffalo River
Little Buffalo River
Percent Finer
0.0
0.2
0.4
0.6
0.8
1.0
10^2
10^3
Grain Size (mm)

Figure 12: (A) Cumulative frequency curves for talus grains at all sites individually in the Boone Formation for both the Main Stem and the Little Buffalo. Percent finer (in decimal form) is on the y-axis and grain size on a log scale is on the x-axis (mm).

(B) Cumulative frequency curves for talus grains at all sites individually in the Everton Formation for both the Main Stem and the Little Buffalo. Percent finer (in decimal form) is on the y-axis and grain size on a log scale is on the x-axis (mm).

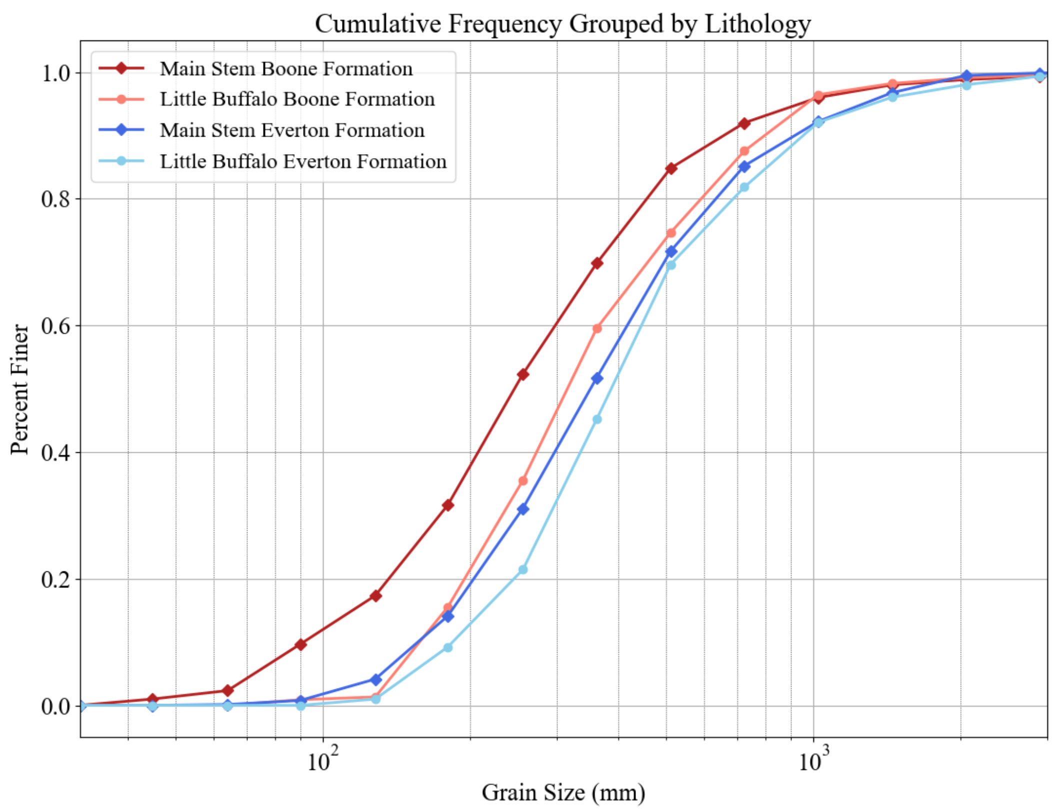

Figure 13: The cumulative frequency curve for all sites of the Main Stem and Little Buffalo and the lithology, Boone Formation or Everton Formation. Percent finer (in decimal form) is on the y-axis and grain size in log scale is on the x-axis (mm). Percent finer is the amount of grains from the sample that are smaller than the grain size indicated.

5.2 Shear Stress

5.2.1 Basal Shear Stress

Whether rivers transport sediment grains depends on the shear stress needed to move each block size at a specific location (Figure 14, 16, 17). I calculated the basal shear stress at each location for three different size flow events (Figure 14). The overall trend going downstream is a decrease in basal shear stress for both the Main Stem Buffalo and Little Buffalo River (Figure 14). During the 2-year flood, basal shear stress was about 120 Pa in the Main Stem Boone Formation while the Main Stem Everton the basal shear stress was about 75 Pa. During a 100-year flood basal shear stress in the Main Stem Boone Formation was about 300 Pa while the Main Stem Everton Formation was about 200 Pa. Those estimated values are the same for the Little Buffalo basal shear stress (Figure 14). The basal shear stress values in the Boone Formation are larger than those in the Everton Formation.

Within the overall trend of generally decreasing basal shear stress going downstream, there were sites with increased shear stress in a spiked pattern (Figure 14). Basal shear stress (Equation 6) is a function of local slope, channel width, and discharge for a particular site location.

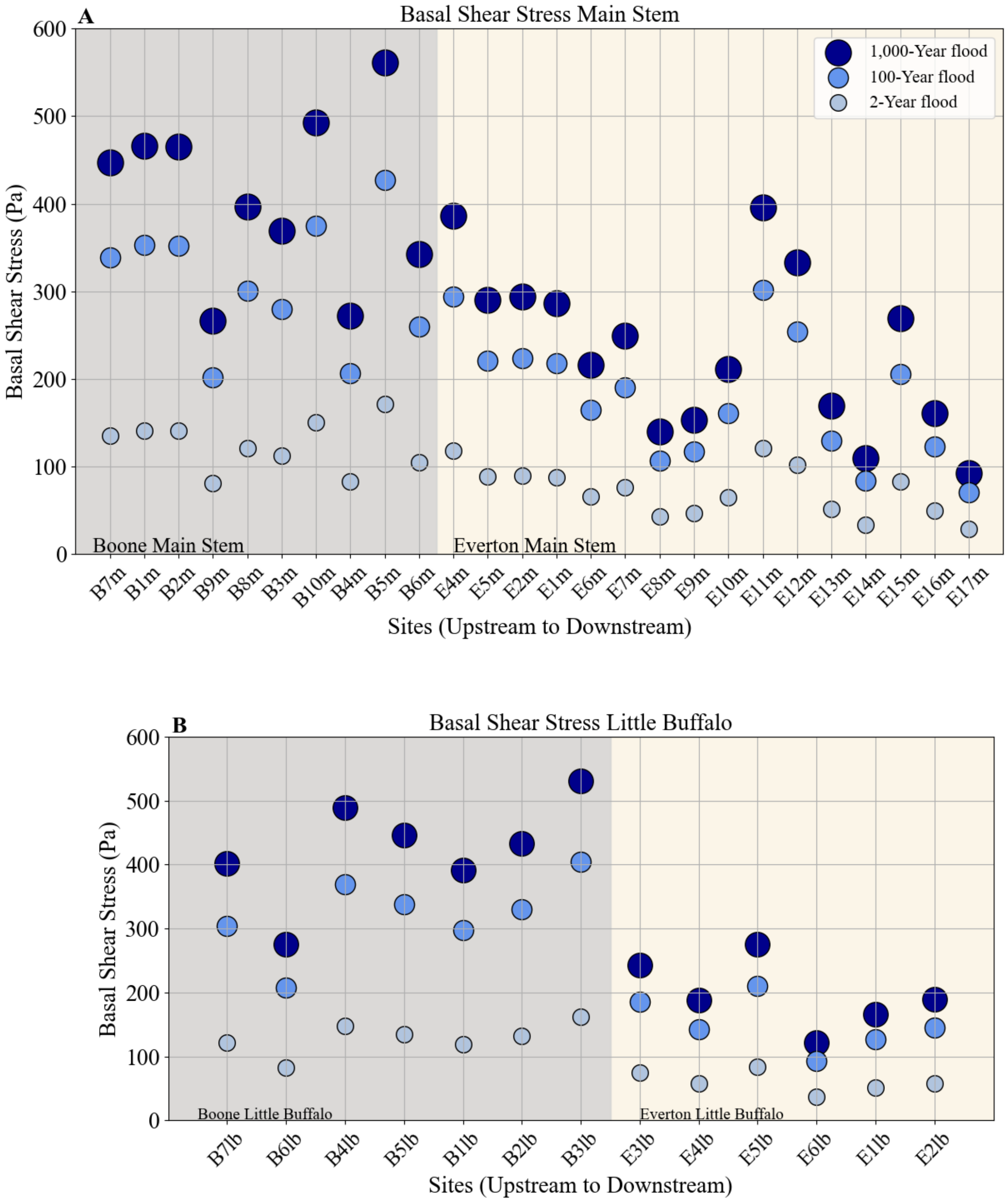

Figure 14: (A) Basal shear stress on the y-axis in Pascals for Main Stem site locations in the upstream to downstream order on the x-axis (unitless). Basal shear stress is a site specific

calculation (Equation 6) using the location discharge of each flood event (2-year, 100-year, and 1,000-year floods), channel width, and slope.

(B) Basal shear stress on the y-axis in Pascals for Little Buffalo site locations in the upstream to downstream order on the x-axis (unitless). Basal shear stress is a site specific calculation (Equation 6) using the location discharge of each flood event (2-year, 100-year, and 1,000-year floods), channel width, and slope.

5.2.2 Excess Shear Stress

Bedload

Potential movement of certain grain sizes (D50 or D84) is seen using excess shear stress, a ratio of basal shear stress to critical shear stress. When the excess shear stress is greater than or equal to one (one being the red line on Figure 15, 16, 17) the threshold of transport is met or exceeded; at this point, sediment grains and talus blocks have the potential to move. If excess shear stress is lower than one, the threshold for potential movement is not met and the block size cannot be transported. We calculated excess shear stress for the D50 and D84 grain sizes in bedload and talus grains for three different flood events. In the 2-year flood, D50 bedload is well above the excess shear stress value of one at nearly every site location (39/40), (Figure 15). Excess shear stress for the D84 bedload grain size is also greater than one at most site locations (29/40) during a 2-year flood, indicating that most bedload grain sizes are transported by the 2-year flood. This also shows that our calculations of basal shear stress for the 2-year flood aligned with previous studies that suggest that most bedload should be transported during 2-year floods (MacKenzie & Eaton, 2017). In the Main Stem, the bedload's ability to move decreases in the downstream direction (Figure 15). The basal shear stress decreases as the discharge increases in both the Main Stem and the Little Buffalo.

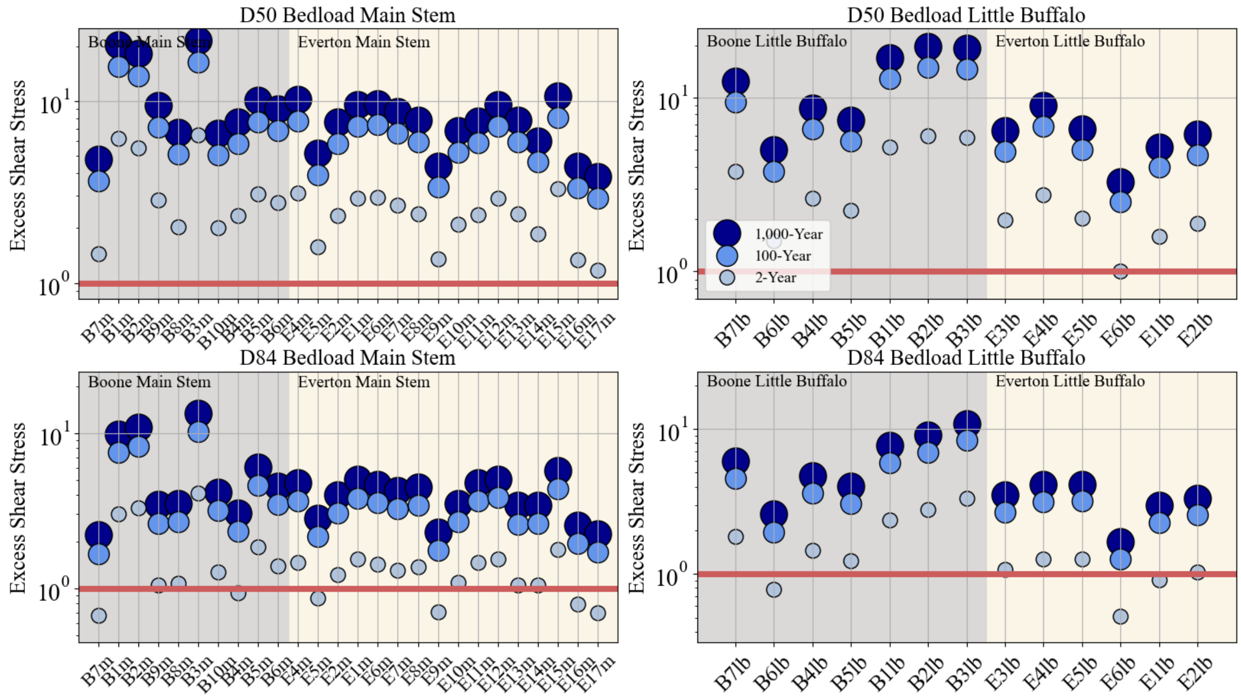

Figure 15: Excess shear stress (basal shear stress/ critical shear stress) on the y-axis for the bedload material on the Main Stem and Little Buffalo site locations in the upstream to downstream order on the x-axis (unitless). Calculations for basal shear stress were made using the 2-year, 100-year, and 1,000-year floods for the D50 and D84 grain sizes per site location. In the upstream reaches the Boone Formation is shown in grey boxes, and in the downstream reaches the Everton Formation is shown in the tan boxes.

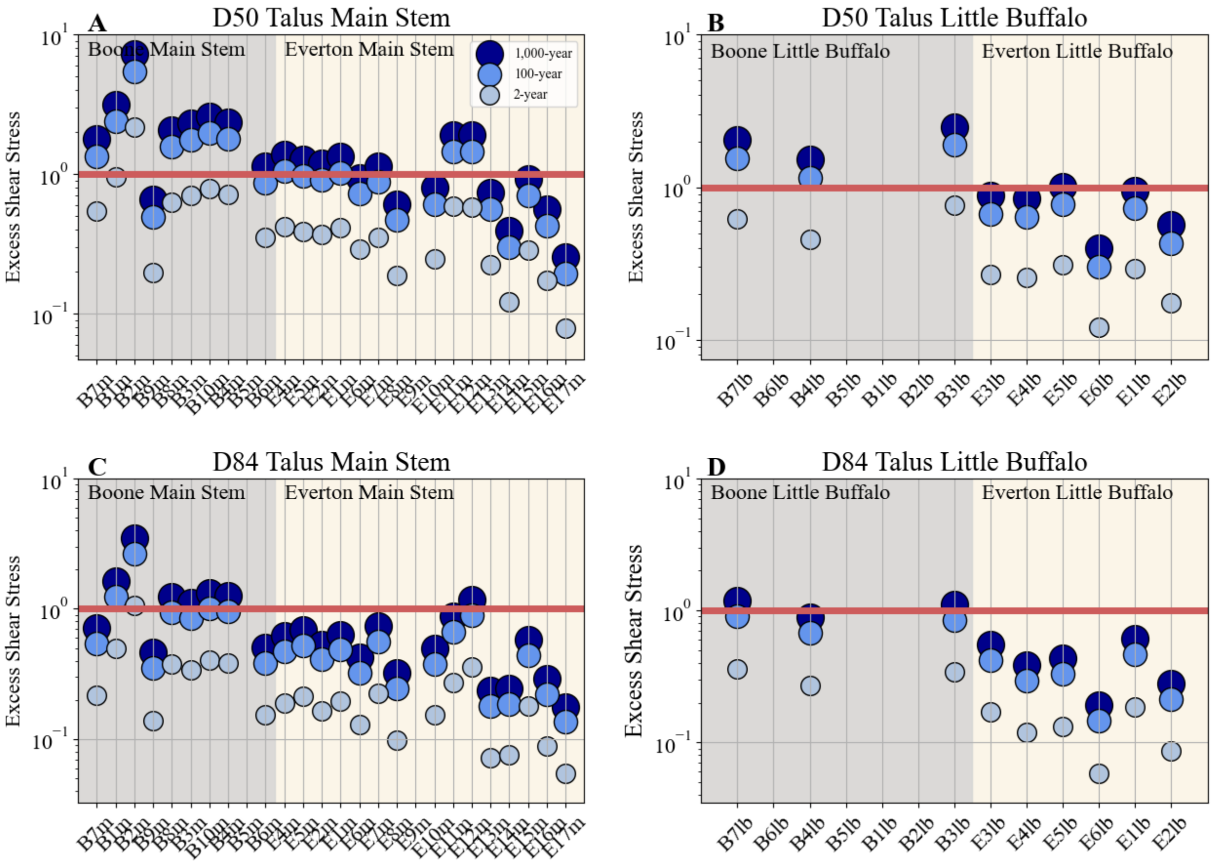

Figure 16: Excess shear stress (basal shear stress/ critical shear stress) on the y-axis for the talus material on the Main Stem and Little Buffalo site locations in the upstream to downstream order on the x-axis (unitless). Calculations for basal shear stress were made using the 2-year, 100-year, and 1,000-year floods for the D50 and D84 grain sizes per site location. In the upstream reaches the Boone Formation is shown in grey boxes, and in the downstream reaches the Everton Formation is shown in the tan boxes.

Talus

Calculated excess shear stresses for talus grains are much smaller than that of the bedload due to much larger talus grain sizes (Figure 16). Talus grains in the Boone Formation generally have higher excess shear stresses than talus grains in the Everton Formation (Figure 16).

For almost every location on the Main Stem Buffalo River and Little Buffalo River, during the 2-year floods, movement is not possible for either the D50 and D84 grain sizes (with the exception of B2m) (Figure 16). No talus grain sizes are potentially transported during the 2-year flood, but talus in the Boone Formation is much closer than the Everton Formation talus.

In the 100-year flood, most of the D50 excess shear stress values in the Boone Formation are above the threshold for potential movement (except for B9m, which only had six very large talus grains). Conversely, in the Everton Formation, only E11m and E12m are potentially moved during the 100-year flood. Most of the D84 excess shear stress values are below the potential movement line except for two locations in the Boone Formation, B1m and B2m (Figure 16C, 16D). Excess shear stresses and the potential for talus transport is higher in upstream reaches, areas of higher local slope, smaller drainage areas, and smaller talus grain sizes in the Boone Formation.

During the 1,000-year flood, the river is able to move almost all of the D50 talus grains of the Boone Formation (with the exception of B9m, also note B9m has only 6 grains). The 1,000-year flood is able to move most of the D84 Boone Formation talus blocks (6/9). In the Everton Formation, however, the 1,000-year flood moves only about half of the D50 grains (7/15). The D84 grain size in the Everton Formation, the largest blocks, are rarely ever moved by the 1,000-year flood (1/15, site E11m). The 1,000-year flood can potentially move more grains in the upstream reaches (Boone Formation) with no possible movement in the downstream reaches (Everton Formation). With no possible movement, the talus grains must weather through time before movement is possible during the 1,000-year flood or be transported during a much larger flood event.

In the Boone Formation and Everton Formation of the Little Buffalo, excess shear stress for the D50 and D84 talus grain sizes was below the threshold line for potential movement in the 2-year flood. Boone Formation D50 and D84 values were closer to the potential movement line than the Everton Formation sites were. The Main Stem and Little Buffalo hold the same trend for the 2-year flood, no movement amongst either lithology, but the Boone Formation's excess shear stress values are higher (closer to the line for potential movement) than those of the Everton Formation.

The Little Buffalo 100-year flood discharge has the ability to move all of the D50 talus grains in the Boone Formation. The discharge was not large enough to move D84 talus in Boone during the 100-year flood, nor the D50 and D84 talus grains of the Everton Formation. The D84 talus in the Boone Formation are closer to the excess shear stress for potential movement than the even the D50 of the Everton Formation are. This means the D84 Everton Formation grains are way below the line for potential movement and will likely be at this location for much longer than the Boone Formation.

The discharge produced by the 1,000-year flood moves D50s of the Boone Formation in the Little Buffalo and some D84s (2/3). In the Everton Formation, only one site (E5lb) has potential movement during the 1,000-year flood. All the other Everton Formation D50 and D84 blocks do not have the potential to move.

I wanted to know what the controlling factor was for these increased shear stress and excess shear stress values was so I did some hypothetical calculations. To determine if excess shear stress is largely controlled by upstream or downstream position, I calculated hypothetical basal shear stress at each location keeping a constant slope of 0.0045 with the field measured channel widths (Figure 17, excess shear stress is basal shear stress divided by critical shear stress). I chose this slope value because this is one of the larger slope values from our data set and I wanted to know if the slope controlled the calculated basal shear stress. I found that a higher slope increased excess shear stress at many of the site locations including those in the Everton Formation. The trend between true measured values and this hypothetical calculation hold similar trends, but the differences are not enough for slope to be the controlling factor on excess shear stress (Figure 17).

I then calculated basal shear stress keeping a constant channel width value of 35 m with the DEM measured slopes per site location (Figure 18). I chose 35 m since it was a lower channel width value and was measured in both the Boone and Everton Formations. These hypothetical calculations show that the talus grain size was the largest influencing factor controlling excess shear stress (Figure 17, 18). If the excess shear stress had been influenced more by slope or channel width in the basal shear stress calculation, we would see a non-uniform change per site location from the original shear stress calculation (Figure 16, 17, 18). No major changes per individual location were observed in the hypothetical calculations, leading me to understand that grain size is the likely control on potential movement in the river aka excess shear stress.

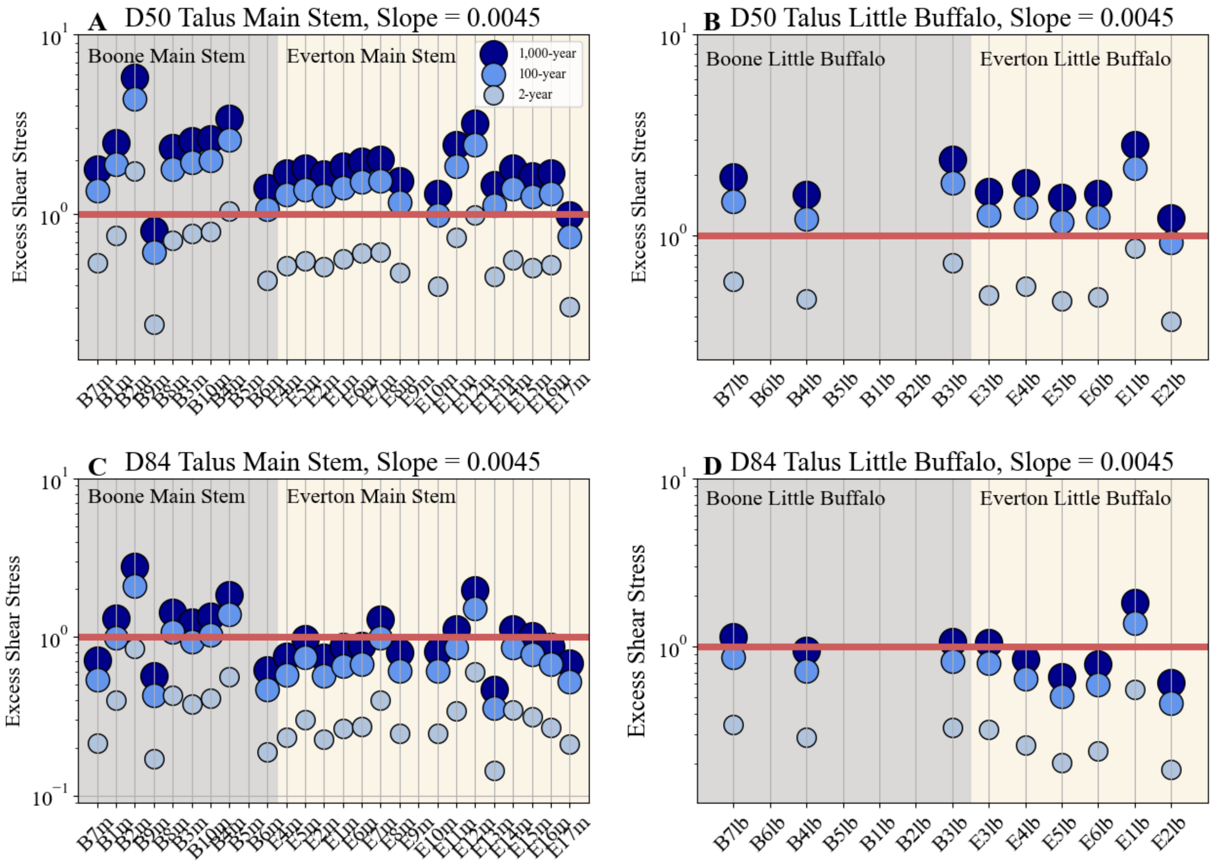

Figure 17: Hypothetical figures for excess shear stress where the slope is constant 0.0045 across the sites and all the measured information staying the same. Testing how much one of our larger slopes would impact the basal shear stress calculations across all sites. Excess shear stress is on the y-axis and site locations in the upstream to downstream order on the x-axis (unitless) for the Main Stem and Little Buffalo. In the upstream reaches the Boone Formation is indicated in a grey box, and in the downstream reaches the Everton Formation is indicated in the tan boxes.

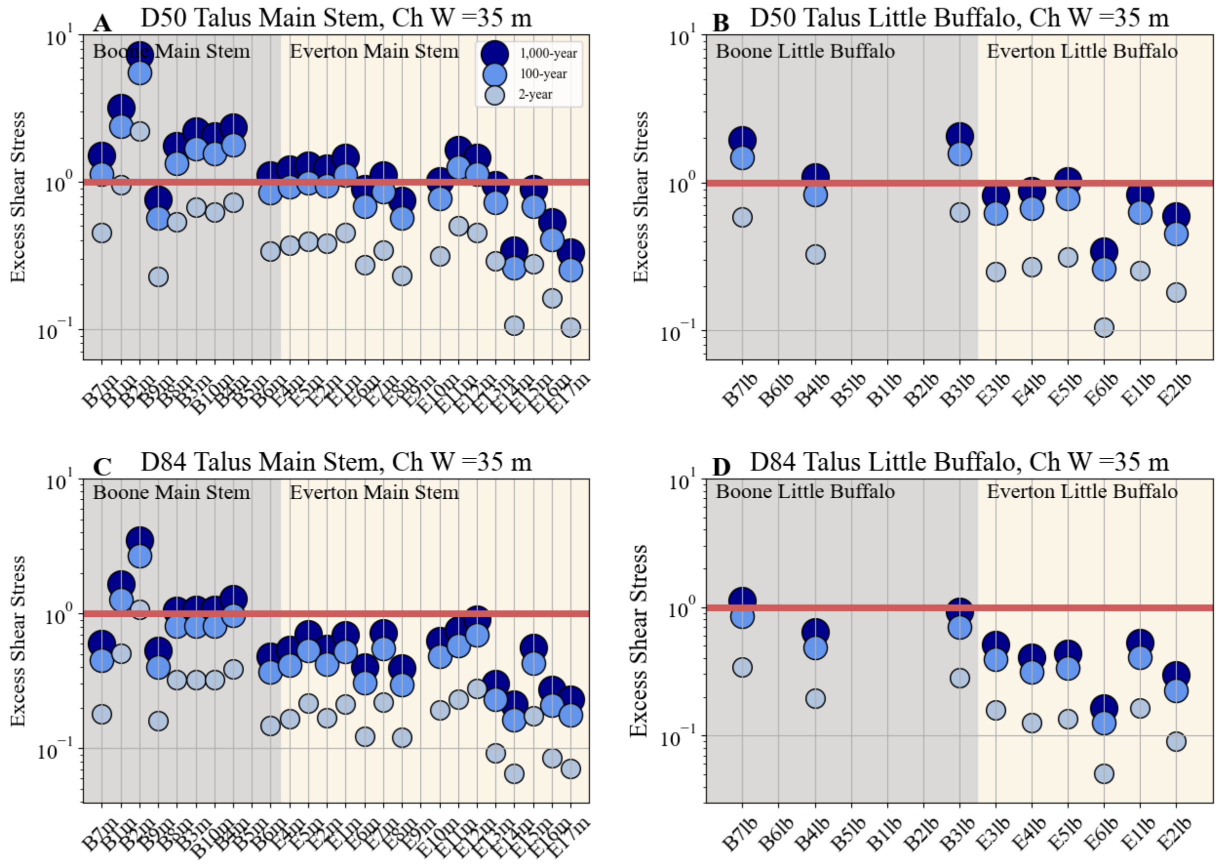

Figure 18: Hypothetical figures for excess shear stress where the channel width is constant 35 m across the sites and all the other measured information stays the same. Testing how much one of our lower channel width would impact the basal shear stress calculations across all sites. Excess shear stress is on the y-axis and site locations in the upstream to downstream order on the x-axis (unitless) for the Main Stem and Little Buffalo. In the upstream reaches the Boone Formation is indicated in a grey box, and in the downstream reaches the Everton Formation is indicated in the tan boxes.

Chapter 6 - **Discussion**

This study presents the field characterization of bedload and talus block size distributions in locations in wide and narrow valleys, as well as calculated shear stress for potential movement of talus blocks of various sizes. In this work, I aim to evaluate two end members of bedrock valley development that may control the rate of valley widening and total valley width.

6.1 Variation in Talus Grain Sizes

The Main Stem Boone Formation talus has more variation and is overall smaller than Everton Formation talus (Figure 11A, 12A, 13). Everton Formation talus is less variable in size and larger than Boone Formation talus (Figure 11A, 12B, 13). Everton Formation talus has a mean grain size of 368 mm and standard deviation of 71 mm. Boone Formation talus has mean grain size of 300 mm and standard deviation of 140 mm. Everton Formation is therefore much less variable in size.

The Little Buffalo River's talus piles follow the same trends as the Main Stem Boone and Everton Formation piles. The Boone Formation talus grains are smaller than the Everton talus grains (Figure 13). In the Boone Formation of the Little Buffalo, four of the seven sites did not have talus, and only three sites did (Figure 11B). This could also suggest that this area has more karst topography potentially providing excess water to the tributary that cannot be considered using drainage area calculations for discharge. Whatever the reason, there are more locations on this large tributary without talus, allowing the river access to the wall for continued lateral erosion.

Variations in grain sizes by lithology can be important to look at, since variation can hint at the mechanisms at work in the river valley. Whatever is controlling the size of the talus blocks in Everton Formation does not change going downstream in the river. This also suggests that Everton Formation blocks do not change size much through time. If they did change over time, many different sizes of talus would be present in piles along the Everton Formation river sites. I may see smaller grains in the Boone Formation because the talus grains weather faster. Boone Formation has a lower chemical resistance than the Everton Formation, if the chert in the Boone Formation is not taken into consideration (Keen-Zebert et al., 2017). Specifically, the limestone lithology in this formation has a high dissolution rate which would allow the talus blocks to become smaller more quickly (Covington et al., 2015).

The Little Buffalo Everton Formation may mirror the Main Stem Everton Formation better than the Boone Formation because there are more sites with talus in the Everton Formation on the Little Buffalo than there are in the Boone Formation. We do not have many sites in the Boone Formation Little Buffalo from which clear comparisons with the Main Stem can be made. Also, variation between the Boone Formation and the Everton Formation in the Little Buffalo does not seem to be as drastic as what we saw in the Main Stem. There are fewer sites in the Little Buffalo than in the Main Stem and the sites are spatially closer to each other, this could explain the smaller variation.

There are two ways that talus grains could arrive at the base of a bedrock cliff. First, talus blocks from both lithologies arrive to the valley bottom in the same size distributions with the Boone Formation weathering at a faster rate. Boone limestone is more soluble than Everton sandstone (Covington et al., 2015; Keen-Zebert et al., 2017). For blocks below the water line, chemical weathering can be a prevalent process. Other below water physical weathering decreases talus block size through abrasion and in river collisions produced by plucking (Whipple et al., 2013; Whipple et al., 2000). Talus that is often above the water line, is weakened through chemical weathering, while the physical weathering occurs from vegetation and trees growing into the blocks followed by cycles of freeze thaw action in cracks. The second option for how talus grains arrive at the base of a bedrock wall are the presence of smaller Boone Formation size distributions and the Everton Formation has larger grain size distributions, with weathering occurring at about the same rate. This idea is supported by differences in fracture spacing. Fracture spacing is a control on the size of blocks released from hillslopes (DiBiase et al., 2018; Sklar et al., 2017; Verdian et al., 2020). Fracture spacing is very much determined by lithology, but there is also an important consideration lithology has on block transport as a control on valley width. In the Buffalo River I observed thinner bedding and smaller fracture spacing in the Boone Formation. Fracture spacing will be further explored in a partnering study at the University of Arkansas that accompanies our large-scale umbrella project, Bedrock Valley Widening in Buffalo National River, headed by Abigail L. Langston. If the Boone Formation produced smaller talus grains they could be small enough for the river to transport quickly. In the Everton Formation the talus grains could be too large to be transported by the river. The size of the talus grain dictates how long that talus grain will be sitting at the base of the bedrock valley wall; we know that larger talus grain would need to sit longer until they are weathered, physically or chemically, to a movable size. In my research I found that the Everton Formation talus was larger than the Boone Formation talus. Unfortunately, with these findings I cannot know what the initial talus block distributions looked like. The two options describing how the talus blocks per lithology fell is equally likely, but to make a better determination toward one arrival method over the other more research would need to be conducted.

6.2 Overlap and Divergence in Talus and Bedload Grain Sizes

Bedload grains represent what a river can regularly transport (Attal et al., 2015). Specifically, gravel bar materials are said to be moved during flood stage discharges (Attal & Lavé, 2006; Parker & Klingeman, 1982). We expect that the relationship between the bedload and talus grain sizes per site location is valuable for understanding how the talus blocks at each site can be potentially moved by the river. Where we see overlap between the largest bedload grains and the smallest talus grains, the talus blocks are closer to potential movement and potentially can be transported. If the D16 talus and the D84 bedload are multiple grain size classes away from each other the river is very unlikely to move talus grains at that discharge level (Figure 11). If the river does not have the potential to move talus blocks, the talus will protect the valley wall from further widening, since we know that the river must be in contact with the valley wall in order to widen the river valley (Hancock & Anderson, 2002).

6.2.1 Overlap

Again, if we see overlap between talus and bedload grain size distributions, I suggest that talus transport is more likely than if a talus grain size distribution is very far from the bedload grain size distribution (Figure 11). Sediment in gravel bars are typically transported during flood events of a certain magnitude (Attal et al., 2015). If the grain size distribution of the sediment in the bedload speaks to what is mobilized, then grains of at least that size are actively transported regularly. For my study, where there is overlap between the largest bedload grains and the smallest talus grains, those talus grains are closer to potential movement and/ or can be potentially transported. If the two distributions are far from each other, movement of talus blocks by the river is also very far away. I also suggest that a talus transport index could be created. An example of that index being: $D84_{bedload}$/ $D16_{talus}$. A created index may correlate with the calculated excess shear stress which could make grain size on its own a very useful measurement for potential talus movement.

The D50 grain size is thought to have first-order control on when bedload sediment begins to move (MacKenzie & Eaton, 2017). The D84 grain size is used to characterize bedload transport of the largest grain sizes in the bedload. Recent studies have shown that D84 is a better representation of the grain size that controls channel morphology and the channel's stability (MacKenzie & Eaton, 2017; MacKenzie et al., 2018). Eaton et al. (2020) discussed the D95 movement threshold of the bedload as having the ability to change the stability of the river channel. If this concept could be brought over to talus piles and bank stability I could determine if the lack of movement by floods stabilizes the channel bank enough to protect the valley wall.

Using the overlap of talus grain size and bedload grain size as a metric for estimating talus block transport is important because one would not need to know the factors that affect sediment transport at a specific site, such as measurements of slope, bankfull width, or drainage area. One can simply say if the distributions overlap, talus transport may be possible at this location. Shear stress calculations for a large number of sites can take a lot of work, especially if the calculations made are for small sections of a stream channel profile. Simply looking at grain size distributions allows us to understand whether talus grains can potentially move without tedious measurements.

6.2.2 Divergence

Moving downstream into the Everton lithology, there is no overlap between the bedload grain distributions and talus grain distributions in both the Main Stem Buffalo River and the Little Buffalo (Figure 11). Some sites furthest upstream are within about 30 to 70 mm (approximately three grain size classes) from the smallest talus grain to the largest bedload grain.

Further downstream there is a divergence between the talus and bedload grain size distributions (approximately six grain size classes). This is due to the bedload grains fining in the downstream direction, not because the talus is getting substantially larger.

If the bedload represents what the river regularly moves, the understanding is that the river moves those bedload grains approximately the size of the D84 often. There is not overlap in the Everton between the bedload and the talus, so we know the talus grains are very unlikely to be moved by the river because the smallest talus grains are several grain size classes larger than the largest bedload grain sizes transported by the river. Simply from looking at the grain sizes of talus and bedload as well as the amount of overlap or divergence between the groups we can estimate how likely the talus blocks are able to be mobilized or the unlikeliness of mobilization. Next, the calculated shear stresses quantify potential movement by the river at specific locations.

6.3 Excess Shear Stress

At each location, I calculated basal shear stress and critical shear stresses for the D50 and D84 grain sizes of the talus blocks (Figure 15). Excess shear stress is $\frac{\tau_0}{\tau_{crit}}$, basal shear stress divided by critical shear stress; when excess shear stress is greater than one, sediment transport is possible. The further away from one in the positive direction, the greater the potential for movement. In both the Main Stem and Little Buffalo River there was a similar trend in potential grain movement. In the Boone Formation with the three flood sizes and two grain sizes chosen most sites could potentially move or were closer to potential movement than the Everton Formation. The grain sizes of the Everton Formation are larger than that of the Boone Formation, but again the lack of excess shear stress is not solely based on grain size but rather a combination of grain size, reduced slope, and channel width going downstream.

The question remains, why is there so much more excess shear stress in the Boone Formation than there is in the Everton Formation? There are more smaller talus grains in the Boone Formation than in the Everton Formation, but the significance of the difference between the total samples per lithology need a statistical comparison to confirm the validity of this basic observation. A t-test comparing all Main Stem Boone Formation talus and all Main Stem Everton Formation talus showed that the Everton Formation talus is significantly and substantially larger than the Boone Formation talus ($p = 1e\text{-}7$). A t-test comparing all Little Buffalo Boone Formation talus and all Little Buffalo Everton Formation talus showed that Everton Formation talus is significantly and substantially larger than the Boone Formation talus ($p = 0.0075$). These two statistical analyses compare the two lithologies per river stretch to better understand the relationship grain size have to each other sample population. Since there is a statistical difference, I have confirmed that block size is a key transport factor and can suggest other factors may be working to move the talus blocks more broadly or controlling block size. In the end this better helps us understand what factors control valley width in conjunction with block size.

More sites in Boone Formation do not have talus grains than sites in the Everton Formation, this is especially prevalent in the Little Buffalo River (Figure 11). This suggests that the talus has been swept away by the river in many places specifically in the Little Buffalo. Movement of the Little Buffalo's talus piles leaves no sites with small talus grains while in the Main Stem there are many piles with small talus grains. At sites in the Little Buffalo where there is no talus there is exposed bedrock wall. In addition, there are slightly higher basal shear stresses in the Little Buffalo Boone Formation compared to the Main Stem Boone Formation. Perhaps this is due to the narrower channel widths seen in the Little Buffalo (Figure 10E, 10F).

The lack of talus piles in the Boone Formation of the Little Buffalo could suggest that the bedrock walls collapse less frequently while the transport of talus by the river stays the same, but this appears unlikely. There is not a way to determine how often walls collapse in either location. The talus grain sizes, however, in the Boone Formation more strongly suggest that river transport is the main mechanism at work moving the talus blocks which would then allow the river access to the bedrock valley wall for continued lateral erosion.

The Boone Formation is present upstream of the Everton Formation indicating that the slope in these stretches are higher than those in the downstream stretches where the Everton Formation exists (Figure 10B, Table 2). I investigated the role of slope and channel width on the excess shear stress for each location in the river (Figure 15A, 15B). By keeping either the slope or the channel width steady each in their own turn, I determined that there is not much of an effect that slope or channel width had independently on the river's ability to move talus grains. I found that the limiting factor is mainly talus grain size.

6.4 Potential Sources of Errors/ Simplifications Made

In my research some simplifications were made due to time constraints, limitations, and other unknowns that exist in our field location. I was able to answer all of my questions in their basic forms to gather valuable data and I are also able to point out where I have made simplifications. This research is under a greater umbrella of academic work performed by Dr. Abigail L. Langston, her PhD student, Clay Robertson, her collaborator Dr. Jill Marshall from University of Arkansas, and Dr. Marshall's graduate students. This means that the research on creating a better understanding of how bedrock river valley widening occurs will continue to be seen in their continued work(s).

Calculated excess shear stresses (Figure 15, 17) are the excess shear stress on the base of the river bed. I applied these excess shear stress calculations to talus blocks that sit on the edges of the channel and are above water during typical low flow conditions. Therefore shear stress needed to move talus blocks is probably higher than I calculated, but the calculations still yield a minimum discharge needed to transport talus blocks. The channel cross sections could have been a valuable measurement to give more accurate shear stress calculations for what the river could move at a particular location in the channel during a particular flood event. A time constraint, safety concern, and overall feasibility of measurement kept me from gathering the channel cross sections at site locations as part of my data set. I decided that making the simplifications of assuming that the talus and bedload are moved by the same cross sectionally averaged shear stress was an adequate simplification for this research project. At the edges not only does vegetation and other roughness elements slow the water, but due to the nature of the channel geometry, the velocity is lower near the river edges, locations where I find our talus piles. While these calculations are likely an underestimation for the shear stress needed to move the talus grains, I determined that the relationship between shear stresses needed to transport talus in the Boone Formation and the Everton Formation is not affected. The shear stress necessary to move talus grains at both locations are equally underestimated.

I also know that I am only characterizing the talus grains that are currently at my site locations. On the river there are a large number of sites that could be measured, but the population can be adequately described by the sample I have collected. I also know that many large flows have occurred in these areas potentially having already moved blocks away. What is left is what was measured. This is true of any field data. Human error along with instrument error is another potential source of incorrect measurement (Bunte et al., 2011; Marcuset al., 1995;

Wohl et al., 1996). In my study only two people collected data, Clay Robertson and Olivia Groeber. We did our best to standardize the data being collected at each site.

6.5 Main Conclusions

These results suggest that talus grain size plays a role in allowing wide valleys to develop and keeping narrow valleys narrow. The river can transport smaller talus grains from the Boone Formation much more rapidly than the Everton Formation, where the talus blocks are larger and less likely to move if weathering on the blocks has not occurred.

In this study, I explored how potential frequency of transport of collapsed talus block material affects the development of wide versus narrow bedrock valleys. I collected data from 40 field locations in the Buffalo River watershed in both wide and narrow valleys. I found:

1. Narrow valleys in the Everton Formation, have larger talus grain sizes than wide valleys in the Boone Formation, that have smaller and more variable talus grain sizes.
2. There is more overlap between the bedload grain sizes and talus grain sizes in the wider valleys, and no overlap in bedload grain sizes and talus grain sizes in the narrow valleys.
3. Excess shear stress calculations show more frequent potential movement in the wide Boone Formation valleys.

These results are important because they help us better understand the mechanisms of talus block movement in a bedrock river valley. If we know how often a talus block can potentially be moved by the river, future research can further explore how quickly those piles are evacuated to better model bedrock river valley widening. More factors are at play when considering how the river widens. Future researchers will have the opportunity to look at the more fine scale details and other factors affecting talus blocks as a bedrock valley wall protection.

References

Attal, M., Mudd, S. M., Hurst, M. D., Weinman, B., Yoo, K., & Naylor, M. (2015). Impact of change in erosion rate and landscape steepness on hillslope and fluvial sediments grain size in the Feather River basin (Sierra Nevada, California). *Earth Surface Dynamics*, *3*(1), 201–222. https://doi.org/10.5194/esurf-3-201-2015

Attal, Mikaël, & Lavé, J. (2006). Changes of bedload characteristics along the Marsyandi River (central Nepal): Implications for understanding hillslope sediment supply, sediment load evolution along fluvial networks, and denudation in active orogenic belts. *Special Paper of the Geological Society of America*, *398*(09), 143–171. https://doi.org/10.1130/2006.2398(09)

Beer, A. R., & Turowski, J. M. (2015). Bedload transport controls bedrock erosion under sediment-starved conditions. *Earth Surface Dynamics*, *3*(3), 291–309. https://doi.org/10.5194/esurf-3-291-2015

Beer, A. R., Turowski, J. M., & Kirchner, J. W. (2017). Spatial patterns of erosion in a bedrock gorge. *Journal of Geophysical Research: Earth Surface*, *122*(1), 191–214. https://doi.org/10.1002/2016JF003850

Beeson, H. W., Flitcroft, R. L., Fonstad, M. A., & Roering, J. J. (2018). Deep-Seated Landslides Drive Variability in Valley Width and Increase Connectivity of Salmon Habitat in the Oregon Coast Range. *Journal of the American Water Resources Association*, *54*(6), 1325–1340. https://doi.org/10.1111/1752-1688.12693

Brocard, G. Y., & Van Der Beek, P. A. (2006). Influence of incision rate, rock strength, and bedload supply on bedrock river gradients and valley-flat widths: Field-based evidence and calibrations from western Alpine rivers (southeast France). *Special Paper of the Geological Society of America*, *398*, 101–126. https://doi.org/10.1130/2006.2398(07)

Bufe, A., Burbank, D. W., Liu, L., Bookhagen, B., Qin, J., Chen, J., … Yang, H. (2017). Variations of Lateral Bedrock Erosion Rates Control Planation of Uplifting Folds in the Foreland of the Tian Shan, NW China. *Journal of Geophysical Research: Earth Surface*, *122*(12), 2431–2467. https://doi.org/10.1002/2016JF004099

Bull, W. B. (1991). *Geomorphic Responses to Climatic Change*. New York: Oxford University Presss.

Bunte, K., Potyondy, J. P., Abt, S. R., & Swingle, K. W. (2011). Discussion of Daniels and McCusker (2010): "Operator bias characterizing stream substrates using Wolman pebble counts with a standard measurement template." Geomorphology 115, 194-198. *Geomorphology*, *134*(3–4), 499–500. https://doi.org/10.1016/j.geomorph.2010.09.020

Covington, M. D., Gulley, J. D., & Gabrovšek, F. (2015). Natural variations in calcite dissolution rates in streams: Controls, implications, and open questions. *Geophysical Research Letters*, *42*(8), 2836–2843. https://doi.org/10.1002/2015GL063044

DiBiase, R. A., Rossi, M. W., & Neely, A. B. (2018). Fracture density and grain size controls on the relief structure of bedrock landscapes. *Geology*, *46*(5), 399–402. https://doi.org/10.1130/G40006.1

Eaton, B. C., MacKenzie, L. G., & Booker, W. H. (2020). Channel stability in steep gravel–cobble streams is controlled by the coarse tail of the bed material distribution. *Earth Surface Processes and Landforms*, *45*(14), 3639–3652. https://doi.org/10.1002/esp.4994

Foster, M. A., Anderson, R. S., Gray, H. J., & Mahan, S. A. (2017). Dating of river terraces along Lefthand Creek, western High Plains, Colorado, reveals punctuated incision. *Geomorphology*, *295*(September 2016), 176–190. https://doi.org/10.1016/j.geomorph.2017.04.044

Fuller et al. (2016). Journal of Geophysical Research: Earth Surface. *Journal of Geophysical Research: Earth Surface*, *121*, 1084–1105. https://doi.org/10.1002/2015JF003728

Goudie, A. S. (2006). The Schmidt Hammer and Related Devices in Geomorphological Research. *Progress in Physical Geography: Earth and Environment*, *14*, 338–345. https://doi.org/10.1016/B978-0-12-374739-6.00398-5

Hancock, G. S., & Anderson, R. S. (2002). Numerical modeling of fluvial strath-terrace formation in response to oscillating climate. *Bulletin of the Geological Society of America*, *114*(9), 1131–1142. https://doi.org/10.1130/0016-7606(2002)114<1131:NMOFST>2.0.CO

Howard, A. D. (1994). A detachment-limited model of drainage basin evolution. *Water Resources Research*, *30*(7), 2261–2285. https://doi.org/10.1029/94WR00757

Hudson, M. R., & Murray, K. E. (2003). Geologic map of the Ponca quadrangle, Newton, Boone, and Carroll Counties, Arkansas. *Newton, Boone, and Carroll Counties, Arkansas: US Geological Survey Miscellaneous Field Studies Map MF–2412, Scale*, *1*(24,000), 80225.

Hudson, M. R., & Turner, K. J. (2007). Geologic Map of the Boxley Quadrangle, Newton and Madison Counties, Arkansas, 1.

Johnson, K. N., & Finnegan, N. J. (2015). A lithologic control on active meandering in bedrock channels. *Bulletin of the Geological Society of America*, *127*(11–12), 1766–1776. https://doi.org/10.1130/B31184.1

Keen-Zebert, A., Hudson, M. R., Shepherd, S. L., & Thaler, E. A. (2017). The effect of lithology on valley width, terrace distribution, and bedload provenance in a tectonically stable catchment with flat-lying stratigraphy. *Earth Surface Processes and Landforms*, *42*(10), 1573–1587. https://doi.org/10.1002/esp.4116

Knighton, D. (1998). *Fluvial Forms and Processes: A New Perspective*. London: Arnold.

Langston, A. L., & Temme, A. J. A. M. (2019). Impacts of Lithologically Controlled Mechanisms on Downstream Bedrock Valley Widening. *Geophysical Research Letters*, *46*(21), 12056–12064. https://doi.org/10.1029/2019GL085164

Langston, A. L., & Tucker, G. E. (2018). Developing and exploring a theory for the lateral erosion of bedrock channels for use in landscape evolution models. *Earth Surface Dynamics*, *6*(1), 1–27. https://doi.org/10.5194/esurf-6-1-2018

Li, T., Fuller, T. K., Sklar, L. S., Gran, K. B., & Venditti, J. G. (2020). A Mechanistic Model for Lateral Erosion of Bedrock Channel Banks by Bedload Particle Impacts. *Journal of Geophysical Research: Earth Surface*, *125*(6), 1–30. https://doi.org/10.1029/2019JF005509

MacKenzie, L. G., & Eaton, B. C. (2017). Large grains matter: contrasting bed stability and morphodynamics during two nearly identical experiments. *Earth Surface Processes and Landforms*, *42*(8), 1287–1295. https://doi.org/10.1002/esp.4122

MacKenzie, L. G., Eaton, B. C., & Church, M. (2018). Breaking from the average: Why large grains matter in gravel-bed streams. *Earth Surface Processes and Landforms*, *43*(15), 3190–3196. https://doi.org/10.1002/esp.4465

Marcotte, A. L., Neudorf, C. M., & Langston, A. L. (2021). Lateral bedrock erosion and valley formation in a heterogeneously layered landscape, Northeast Kansas. *Earth Surface Processes and Landforms*, *46*(11), 2248–2263. https://doi.org/10.1002/esp.5172

Marcus, W. A., Ladd, S. C., Stoughton, J. A., & Stock, J. W. (1995). Pebble counts and the role of user-dependent bias in documenting sediment size distributions. *Water Resources Research*, *31*(10), 2625–2631.

Marshall, J. A., Roering, J. J., Bartlein, P. J., Gavin, D. G., Granger, D. E., Rempel, A. W., … Hales, T. C. (2015). Earth Sciences: Frost for the Trees: Did climate increase erosion in unglaciated landscapes during the late Pleistocene? *Science Advances*, *1*(10). https://doi.org/10.1126/sciadv.1500715

Marshall, J. A., & Sklar, L. S. (2012). Mining soil databases for landscape-scale patterns in the abundance and size distribution of hillslope rock fragments. *Earth Surface Processes and Landforms*, *37*(3), 287–300. https://doi.org/10.1002/esp.2241

May, C., Roering, J., Eaton, L. S., & Burnett, K. M. (2013). Controls on valley width in mountainous landscapes: The role of landsliding and implications for salmonid habitat. *Geology*, *41*(4), 503–506. https://doi.org/10.1130/G33979.1

Menting, F., Langston, A. L., & Temme, A. J. A. M. (2015). Downstream fining, selective transport, and hillslope influence on channel bed sediment in mountain streams, Colorado Front Range, USA. *Geomorphology*, *239*, 91–105. https://doi.org/10.1016/j.geomorph.2015.03.018

Montgomery, D. R. (2004). Observations on the Role of Lithlogy in Strath Terrace Formation and Bedrock Channel Width. *American Journal of Science*, *304*, 454–476.

Moore, D. (2014). Frequency Curve Determination Version 306.xlsm. Natrual Resources Conservation Service.

Parker, G., & Klingeman, P. C. (1982). On Why Gravel Bed Streams Are Paved, *18*(5), 1409–1423.

Sampson, C. C., Anderew, M. S., Bates, P. D., Neal, J. C., Alfieri, L., & Freer, J. E. (2015). Water Resources Research. *Journal of the American Water Resources Association*, *51*(3), 7358–7381. https://doi.org/10.1111/j.1752-1688.1969.tb04897.x

Schanz, S. A., & Montgomery, D. R. (2016). Lithologic controls on valley width and strath terrace formation. *Geomorphology*, *258*, 58–68. https://doi.org/10.1016/j.geomorph.2016.01.015

Schanz, S. A., Montgomery, D. R., Collins, B. D., & Duvall, A. R. (2018). Multiple paths to straths: A review and reassessment of terrace genesis. *Geomorphology*, *312*, 12–23. https://doi.org/10.1016/j.geomorph.2018.03.028

Sklar, L. S., & Dietrich, W. E. (2001). Sediment and rock strength controls on river incision into bedrock. *Geology*, *29*(12), 1087–1090. https://doi.org/10.1130/0091-7613(2001)029<1087:SARSCO>2.0.CO

Sklar, L. S., & Dietrich, W. E. (2004). A mechanistic model for river incision into bedrock by saltating bed load. *Water Resources Research*, *40*(6), 1–22. https://doi.org/10.1029/2003WR002496

Sklar, L. S., Riebe, C. S., Marshall, J. A., Genetti, J., Leclere, S., Lukens, C. L., & Merces, V. (2017). The problem of predicting the size distribution of sediment supplied by hillslopes to rivers. *Geomorphology*, *277*, 31–49. https://doi.org/10.1016/j.geomorph.2016.05.005

Snyder, N. P., Whipple, K. X., Tucker, G. E., & Merritts, D. J. (2003). Importance of a stochastic distribution of floods and erosion thresholds in the bedrock river incision problem. *Journal of Geophysical Research: Solid Earth*, *108*(B2). https://doi.org/10.1029/2001jb001655

Sweeney, B. W., Bott, T. L., Jackson, J. K., Kaplan, L. A., Newbold, J. D., Standley, L. J., … Horwitz, R. J. (2004). Riparian deforestation, stream narrowing, and loss of stream ecosystem services. *Proceedings of the National Academy of Sciences of the United States of America*, *101*(39), 14132–14137. https://doi.org/10.1073/pnas.0405895101

Thaler, E. A., & Covington, M. D. (2016). The influence of sandstone caprock material on bedrock channel steepness within a tectonically passive setting: Buffalo National River Basin, Arkansas, USA. *Journal of Geophysical Research: Earth Surface*, *121*(9), 1635–1650. https://doi.org/10.1002/2015JF003771

Tomkin, J. H., Brandon, M. T., Pazzaglia, F. J., Barbour, J. R., & Willett, S. D. (2003). Quantitative testing of bedrock incision models for the Clearwater River, NW Washington State. *Journal of Geophysical Research: Solid Earth*, *108*(B6). https://doi.org/10.1029/2001jb000862

Tucker, G. E., & Bras, R. L. (2000). variability in drainage basin evolution • = P. *Water Resources*, *36*(7), 1953–1964.

Turowski et al. (2008). Distribution of erosion across bedrock channels. *Earth Surface Processes and Landforms*, *33*(July), 353–363. https://doi.org/10.1002/esp

U. S. Geological Survey. (2020). Elevation Products (3DEP). Retrieved from https://apps.nationalmap.gov/downloader/#/

USGS. (2022). Discharge Data. Retrieved from https://waterdata.usgs.gov/nwis/wys_rpt?dv_ts_ids=3423&wys_water_yr=2021&site_no=07056000&agency_cd=USGS&adr_water_years=2006%2C2007%2C2008%2C2009%2C2010%2C2011%2C2012%2C2013%2C2014%2C2015%2C2016%2C2017%2C2018%2C2019%2C2020%2C2021&referred_module=

Verdian, J. P., Sklar, L. S., Riebe, C. S., & Moore, J. R. (2020). Sediment size on talus slopes correlates with fracture spacing on bedrock cliffs: Implications for predicting initial sediment size distributions on hillslopes. *Earth Surface Dynamics*, *9*(4), 1073–1090. https://doi.org/10.5194/esurf-9-1073-2021

Whipple et al. (2013). 9.28 Bedrock Rivers, *9*, 550–573.

Whipple, K. X., Hancock, G. S., & Anderson, R. S. (2000). River incision into bedrock: Mechanics and relative efficacy of plucking, abrasion, and cavitation. *Bulletin of the Geological Society of America*, *112*(3), 490–503. https://doi.org/10.1130/0016-7606(2000)112<490:RIIBMA>2.0.CO;2

Whipple, Kelin X., & Tucker, G. E. (1999). Dynamics of the stream-power river incision model: Implications for height limits of mountain ranges, landscape response timescales, and research needs. *Journal of Geophysical Research: Solid Earth*, *104*(B8), 17661–17674. https://doi.org/10.1029/1999jb900120

Wohl, E. E., Anthony, D. J., Madsen, S. W., & Thompson, D. M. (1996). A comparison of surface sampling methods for coarse fluvial sediments. *Water Resources Research*, *32*(10), 3219–3226. https://doi.org/10.1029/96WR01527

Yanites, B. J. (2018). The Dynamics of Channel Slope, Width, and Sediment in Actively Eroding Bedrock River Systems. *Journal of Geophysical Research: Earth Surface*, *123*(7), 1504–1527. https://doi.org/10.1029/2017JF004405

Yanites, B. J., Tucker, G. E., Mueller, K. J., Chen, Y. G., Wilcox, T., Huang, S. Y., & Shi, K. W. (2010). Incision and channel morphology across active structures along the Peikang River, central Taiwan: Implications for the importance of channel width. *Bulletin of the Geological Society of America*, *122*(7–8), 1192–1208. https://doi.org/10.1130/B30035.1

Zunka, J. P. P. (2018). Controls on Process and Form in Alluvial and Bedrock Meandering Rivers. *Oregon State University*.